CODEN:LUTEDX/(TEIE-5357)/1-61/(2015)

IndustrialElectricalEngineeringandAutomation

Sensorless Control for Dynamic Testing of PMSMs

Henrik Rydin Malmqvist

Division of Industrial Electrical Engineering and Automation Faculty of Engineering, Lund University

Sensorless Control for Dynamic Testing of Permanent Magnet Synchronous Machines

Henrik Rydin Malmqvist

June 25, 2015

Abstract

This thesis investigates if it is possible to use the dynamic braking test method together with sensorless control. A literature study is conducted about different sensorless methods in order to find methods that fits the application. From the litterature study are two sensorless methods implemented and simulated in Matlab Simulink. The results from the simulations shows that when using the two methods together it is possible to test a PMSM in all possible current combinations. However for some current combinations are the rotor position estimation not perfect which leads to less accuracy for the results from the dynamic braking test method.

Contents

1 Introduction

In this section are background information, scope, goals and method presented.

1.1 Structure of the thesis

This thesis starts with a short background and description of the problem, later follows the project goals for solving the problem. Then a short theoretical introduction is given to provide the reader some basic information. After that, a description over what has been conducted and results from the simulations are presented. The last part of the report contains a conclusions section, future work and a reference list.

1.2 Background

According to the UNFCCC, the climate change is the most important challenge to solve for the survival of mankind. UNFCCC also states that the human contribution to the climate change by burning fossil fuel is significant, the transportation on land accounts for 13.1% of the total emission of green-house gases from human activity [1]. To reduce the emission of green-house gases from vehicles, the European Union has made legislations that set standards to regulate the green-house gas emission from new vehicles [2]. To meet up to those standards, the automotive industry has started to look at bio-fueled, hybrid electric, electrical and hydrogen vehicles [3]. In the last three solutions it is required to equip the vehicle with electrical machines for propulsion and regeneration.

When the electrical machines are becoming more common in vehicle applications, it is getting more and more important for the automotive industry to find easy ways of testing electrical machines. As an answer to that matter, the Industrial Electrical engineering and Automation division at Lund University is working on a project that aims to investigate and develop a new method for testing electrical machines [4]. The advantages with the new method are that it is less time consuming and no torque sensor or breaking machine are needed during the testing [4]. A typical test sequence with the new method is that the machine is accelerated to a pre-defined speed and when that speed is reached, it is braked and accelerated to the same speed in the opposite rotational direction [5].

Usually, to control a PMSM efficiently the information about the rotor position is needed [6]. The more conventional way to obtain the rotor position is to use a rotor position sensor. Because of some drawbacks with using rotor position sensors such as calibration, it was decided that the ability of using sensorless control in the dynamic test bench should be investigated.

1.3 Project goals

The project goals were set up to make it possible to verify if this thesis is solving the problem that was formulated above.

- Define the requirements that the sensorless control strategy needs to fulfill in order to be used in dynamic testing.
- Conduct a literature study to identify which different sensorless control strategies that exist and evaluate their advantages and drawbacks regarding the test application.
- Research and decide which sensorless control method or methods could be suitable to be used in the new testing method that is under development regarding the demands for the test method.
- Implement a simulation model with regards to evaluate if the sensorless control method gives satisfying results.

1.4 Method

This project starts with literature study of the new dynamic test method for PMSMs. A specification list is created that contains the needs and demands on a new sensorless control method for the new dynamic test method application.

A literature study is conducted on different sensorless control methods for PMSMs. In order to start the literature study two articles containing an overview of different techniques for sensorless control methods are read. Then the techniques that are estimated to fit to the application are investigated more carefully.

The sensorless control methods that are expected to fit the dynamic test application are implemented in Matlab Simulink in order to see if they work. In Matlab Simulink the implemented sensorless methods are used in the dynamic test method application and the results are compared with results obtained with rotor position sensor.

1.5 Limitations of the master project

This project focuses on giving a suggestion on a sensorless control method that can be used for the new testing method. Only the methods that are chosen from the literature study are simulated, in other words this thesis does not aim to simulate and compare different sensorless control methods. To evaluate if the sensorless method is useful in this application, only simulations in Matlab Simulink are conducted and the machines fluxes and torque production are calculated by the new test method.

The limitations of the simulation model are depending on the simplified PMSM model that is used in Matlab Simulink. Since the flux maps that are used in the model are obtained from a real PMSM, it can be concluded that the model is acting as a real motor as long as the currents are with in the area of the

flux maps. Some deviations for the PMSM can be assumed to depend on the resolution of the flux maps. The whole model is simulated in continuous time but some parts such as the PI-controllers and digital filters works in discrete time.

2 The PMSM

In this section some fundamentals about the PMSM and the modeling of the PMSM are presented. The information in this section can be found in many different books for electrical engineers such as [6] and [7].

The PMSM is usually a three phase electrical machine with windings in the stator and permanent magnets in the rotor. Since the PMSM is a synchronous machine the velocity of the rotor follows the frequency of the current it is fed with divided by number of pole pairs in the machine.

2.1 Transformations of a three phase system

The PMSM is often modeled in the two phase rotating reference frame, but in reality most PMSMs are 3 phase electrical machines. In order to go from a 3 phase system to a 2 phase system different transformations have to be done and they are explained below.

A 3 phase system contains three vectors abc, that are shifted 120 degree between each other, see figure 1. One way to represent those three vectors is by taking the resulting vector of the 3 phase system and divide it into two components aligned with the alpha and beta axis again, see figure 1. The alpha beta system contains therefor two vectors that are changing amplitude in order to recreate the resulting vector of the 3 phase system.

In some cases it can be unpractical to calculate with vectors that is varying its amplitude so therefor a way of representing the 3 phase system with just two axes called d and q respectively is used. In figure 1, to the left shows the dq axes versus the alpha beta axes. The dq vectors are instead of changing amplitude, rotating counterclockwise with the electrical angular frequency to recreate the resulting vector of the alpha beta system. The dq frame is due to its rotation also referred to as the rotating reference frame.

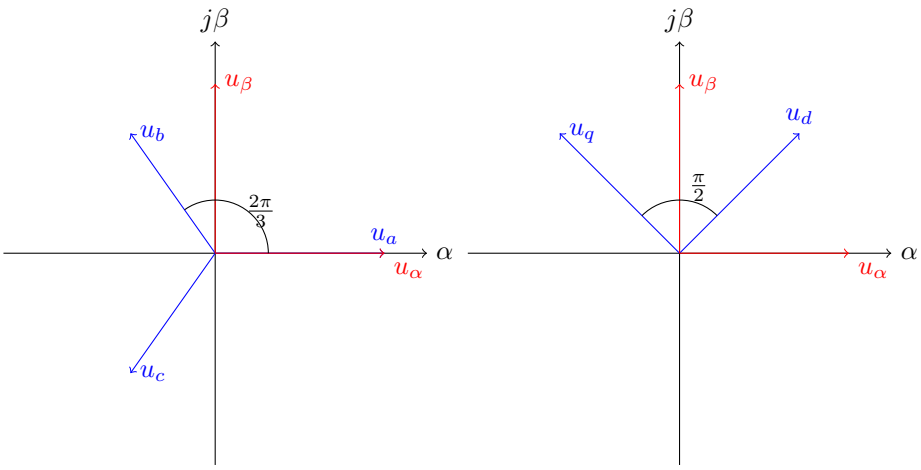

Figure 1: abc representation versus α β and α β representation versus the dq representation.

The matrix in equation 1 shows the transformation from 3-phase-system towards 2 phase stationary reference frame α β representation. In equation 2 the inverse transformation is presented.

$$\begin{bmatrix} u_\alpha \\ u_\beta \end{bmatrix} = \begin{bmatrix} \frac{2}{3} & -\frac{1}{3} & -\frac{1}{3} \\ 0 & \frac{1}{\sqrt{3}} & -\frac{1}{\sqrt{3}} \end{bmatrix} \begin{bmatrix} u_a \\ u_b \\ u_c \end{bmatrix} \tag{1}$$

$$\begin{bmatrix} u_a \\ u_b \\ u_c \end{bmatrix} = \begin{bmatrix} 1 & 0 \\ -\frac{1}{2} & \frac{\sqrt{3}}{2} \\ -\frac{1}{2} & -\frac{\sqrt{3}}{2} \end{bmatrix} \begin{bmatrix} u_\alpha \\ u_\beta \end{bmatrix} \tag{2}$$

Equation 3 shows the transformation from α β representation to dq representation.

$$\begin{bmatrix} u_d \\ u_q \end{bmatrix} = \begin{bmatrix} cos(\theta) & sin(\theta) \\ -sin(\theta) & cos(\theta) \end{bmatrix} \begin{bmatrix} u_\alpha \\ u_\beta \end{bmatrix} \tag{3}$$

The inverse transform, from dq rotating reference frame to $\alpha\beta$ representation is shown in equation 4.

$$\begin{bmatrix} u_\alpha \\ u_\beta \end{bmatrix} = \begin{bmatrix} cos(\theta) & -sin(\theta) \\ sin(\theta) & cos(\theta) \end{bmatrix} \begin{bmatrix} u_d \\ u_q \end{bmatrix} \tag{4}$$

2.2 Modeling of the PMSM

The PMSM is usually modeled in the rotating reference frames, in Krishnans book about PMSMs two equivalent circuits are presented, one dynamic and one in steady state including the iron losses [6].

Dynamic equivalent model

The equivalent dynamic circuit is shown in figure 2, the resistor represents the voltage drop over the windings which is due to the resistance in the wire the winding is built from [6]. After the resistor follows the inductance which models the induced voltage from variations in the flux linkage [6]. Finally the induced voltage is depending on the flux produced in the other axis which is showed in figure 2 [6].

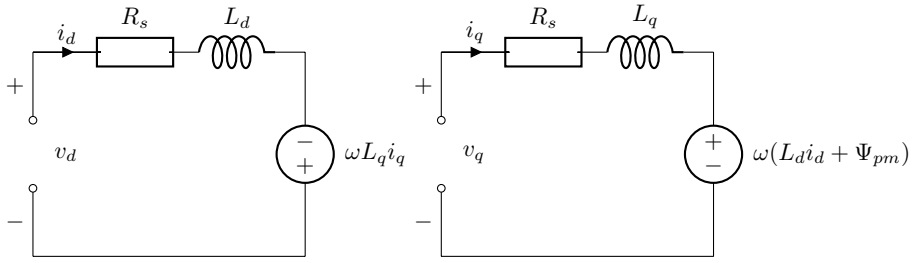

Figure 2: Equivalent dynamic circuits for the d- and q-frame.

The voltage equation for the d-frame consists of three parts see equation 5. The first part shows the voltage drop over the windings represented by R_s. The second term shows the induced voltage from the winding in the same axis. Finally is the cross coupling term which consists of the induced voltage due to the flux produced from the windings and current in the q-axis [6].

$$v_d = R_s i_d + L_d \frac{di_d}{dt} - \omega L_q i_q \tag{5}$$

The equation for the q-voltage is shown in equation 6, notice that the q-voltage equation is similar to the d-voltage, only the voltage sign and the third term is different and that is due to the flux created by the permanent magnets in the rotor [6].

$$v_q = R_s i_q + L_q \frac{di_q}{dt} + \omega(L_d i_d + \Psi_{pm}) \tag{6}$$

The linked fluxes are given by equation 7 and 8 [6]. The d-axis flux consists of two terms where the first one is the flux created by the current and winding in the d-frame and the second term is the flux that is created by the permanent magnets. The flux that is created in the q-axis is directly from the current and the winding in the q-axle.

$$\Psi_d = L_d i_d + \Psi_{pm} \tag{7}$$

$$\Psi_q = L_q i_q \tag{8}$$

Steady state equivalent model including iron losses

Since the dynamic test method only works when the motor is operating in steady state mode, the equivalent circuit can be simplified by removing the inductance [5]. In the equivalent circuit a resistance is also added in parallel to the voltage drop and that is to represent the iron losses in the motor. Because of the dynamic test method structure with a voltage subtraction the iron losses will disappear. This make calculations possible without knowing motor parameters more about later in this thesis [5]. The steady state equivalent circuits are shown in figure 3.

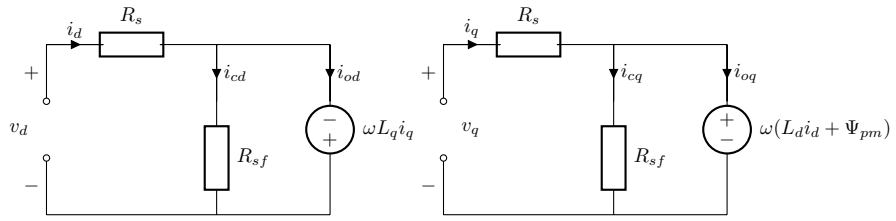

Figure 3: Equivalent steady state circuits with core losses for the d- and q-frame.

From the steady state equivalent circuits in figure 3 have the voltage equations that is shown in equation 9 and 10 been derived [8].

$$v_d = R_s i_d - \omega L_q i_{oq} \tag{9}$$

$$v_q = R_s i_q + \omega L_d i_{od} + \omega \Psi_{pm} \tag{10}$$

The currents in the equivalent circuits are given by equation 11 and 12 below that can be obtained by simple current division [8].

$$i_{od} = i_d - i_{cd} = i_d - \frac{\omega L_q i_{oq}}{R_{df}} \tag{11}$$

$$i_{oq} = i_q - i_{cq} = i_q - \frac{\omega L_d i_{od} + \omega \Psi_{pm}}{R_{qf}} \tag{12}$$

By combining equation 9, 10, 11 and 12 the equivalent circuit voltages can be written as shown in equation 15 and 16 [8].

$$v_d = (R_s + \frac{\omega^2 L_d L_q}{R_{sf}}) i_d - \omega \Psi_q + \frac{\omega^2 L_q \Psi_{pm}}{R_{sf}} \tag{13}$$

$$v_q = (R_s + \frac{\omega^2 L_d L_q}{R_{sf}}) i_{sq} + \omega \Psi_d \tag{14}$$

In the equivalent steady state circuit the core losses are modeled as a resistor in parallel with the motor. The core losses are mainly hysteresis losses and eddy current losses [6].

Hysteresis losses occurs when a magnetic field has been affecting a ferromagnetic material. Then some of the dipoles are still aligned in the direction of the magnetic field even though it has been removed. The losses occur because it costs more energy to align those dipoles that are still align with the old magnetic field in another direction[6].

Eddy current losses occurs when the iron is exposed to varying fluxes and then an induced emf is created that generates a current in the opposite direction which costs energy [6]. The eddy current losses depends on the material in the core and is proportional to the electrical frequency.

In [9] a third source of core losses is introduced as excess losses and it is also like the other two loss components depending on the material and the electrical frequency. Below is the full equation for core losses presented according to [9] in equation 17.

$$P_{fe} = k_h \omega B_m^{\beta} + k_c (\omega B_m)^2 + k_e (\omega B_m)^{1.5} \tag{15}$$

Since the motor is a three phase motor the resistor is given in equation 16 [5]. However because of the design of the dynamic test method the iron loss resistance will never be calculated in the test method.

$$R_f = 3\frac{(\omega \Psi_{pm})^2}{P_{fe}} \tag{16}$$

2.3 Torque creation of the PMSM

The electrical machine is created to convert electrical energy to mechanical energy or vice versa. There are two ways for a salient pole PMSM to generate torque [6].

The first torque producing component in the PMSM is presented here. A varying magnetic field created by the stator windings. Because of the materials in the PMSMs rotor and their magnetic permeability the rotor is moved by the magnetic field to a position where the reluctance for the magnetic field lines is smaller. By varying the magnetic field that is created by the stator inductances the rotor will follow the field in order to reduce the reluctance and torque is produced [6].

The second way for the PMSM to create torque is by using the windings in the stator to create a rotating magnetic fields then the permanent magnets in the rotor will follow the magnetic field in the stator so that the magnetic angle between the stator and rotor will be kept near 0 degree.

From the torque equation it is possible to see the above mentioned ways of creating torque in the PMSM see equation 17. The first part only depends on the permanent magnets magnetization and the second part of the equation

depends on the reluctance differences between the two axes. In equation 17 T_e stands for the electromagnetic Torque, p stands for the number of magnetic poles in the machine, ψ_{pm} stands for the permanent magnets flux, i_s stands for the magnitude of the currents in both d and q axes in the stator, δ stands for the torque angle, L_d and L_q stands for the inductance of the two axes.

$$T_e = \frac{3}{2}\frac{p}{2}\Big[\psi_{pm} i_s sin(\delta) + \frac{1}{2}(L_d - L_q) i_s^2 sin(2\delta)\Big](Nm). \tag{17}$$

Since the PMSM is a synchronous machine the rotor speed depends directly on the frequency of the currents it is fed with and the number of pole pairs of the motor [6]. The rotor speed is shown in equation 2 where p stands for the number of pole pairs in the motor, the f stands for the electrical frequency.

$$\omega = \frac{4\pi f}{p}(rad/s). \tag{18}$$

2.4 The inverter for the PMSM

In order to run the PMSM at different speeds a device that can feed the PMSM with voltages at varying frequency is needed. In order to do so a two level voltage source PWM inverter is selected.

The inverter uses switches that turn on and off DC voltages with a high frequency to create three phase voltages with variable frequency. The inverter that is used in the Simulink model is a 3 phase 2 levels inverter. Which means that for every phase the inverter can give two voltage levels $V_{dc}/2$ and $-V_{dc}/2$. To create the desired voltage the inverter uses the reference signal from the current controller and a high frequent triangular wave. When the reference signal is above the triangle wave then the switch is on and gives $V_{dc}/2$ and the switch gives $-V_{dc}/2$ when the reference signal is below the triangle wave, see figure 4.

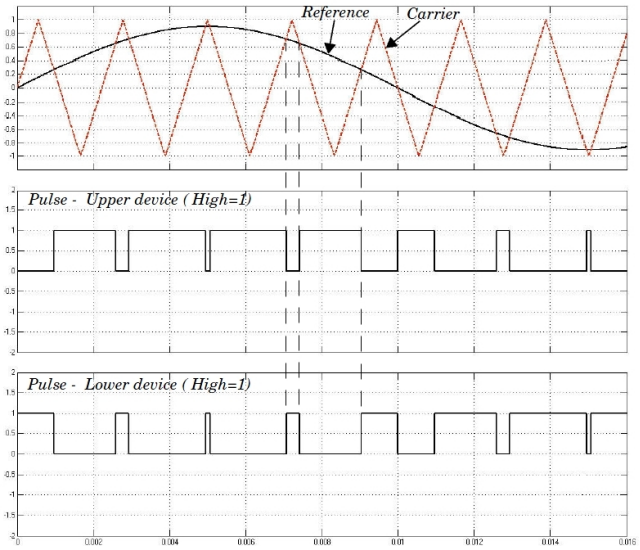

Figure 4: Shows how the inverter creates a voltage from a triangle wave and a reference wave. From: `http://se.mathworks.com/help/physmod/sps/powersys/ref/pwmgenerator.html`

The frequency of the triangular wave has to be at least 10 times the frequency of the reference signal if the inverter should be able to create the correct output signal from the reference [7].

3 Dynamic testing of PMSMs

The procedure for the test method is presented in figure 5, where the green line is the q current, the blue line is the d current and the red line is the speed.

The method consists of a speed sequence that has to be performed. The speed sequence starts accelerate the machine to a negative pre-defined speed see the bottom left corner of the square in figure 5. Then the machine is braked to zero speed and directly accelerated up to the pre-defined positive speed see the upper right corner of square in figure 5.

When performing the test method the measurements of speed voltages and currents are needed, the measurements takes place when the test procedure is within the black square in figure 5.

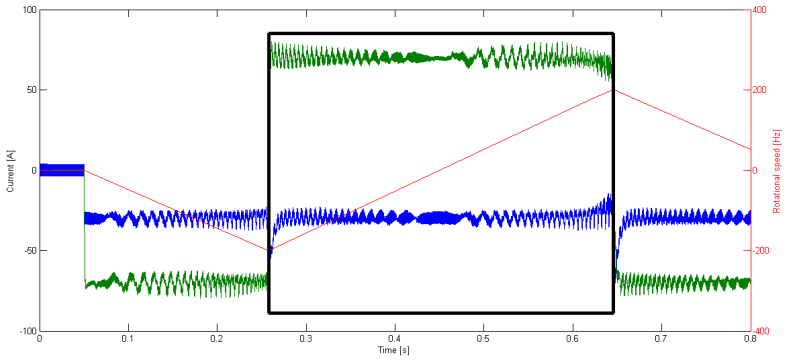

Figure 5: Test sequence when the new test method is performed, only the measurements inside the rectangle are relevant for the test method.

The test method can be used to measure the linked stator fluxes. The dynamic test method consists of two methods to calculate torque, using voltages and speed or by using the moment of inertia and acceleration.

3.1 Flux and Torque calculation using voltage and current

This method builds directly on the steady state equivalent model with core losses and uses the voltage equations derived from that circuit.

From the voltage measurements during the test sequence when it is within the square in figure 5, and are used according to the following equations on the next page. When calculating the linked stator flux for the d-vector the voltage over the q-axis is used and the measurement for when the machine is accelerating is subtracted with the measurement for when the machine is braked for each speed. After the subtraction, the remaining parts of the voltage equation from the steady state equivalent circuit are the second term that contains the speed and the linked stator flux. Since an addition has been performed and both voltages are at same speed the result is 2 times the speed times the linked

stator flux in the d-axis. In order to get the linked stator flux the equation is divided by 2 times the speed see equation 19.

$$\Psi_d = \frac{v_q^{\omega} - v_q^{-\omega}}{2\omega} \tag{19}$$

In order to get the stator flux linkage in the q axis similar calculations are performed as in equation 19 the only difference is that the voltage during braking is being subtracted by the voltage during acceleration see equation 20. The reason for the change in position of the voltages is due to the second term in the voltage equation for the d voltage is negative see equation 9 and 10.

$$\Psi_q = \frac{v_d^{-\omega} - v_d^{\omega}}{2\omega} \tag{20}$$

In order to be able to calculate the torque that is produced by the electrical machine the currents are needed and they are assumed to be the mean value of the current for each speed when the machine is braking and accelerating.

Since the machine is held in steady state during the sequence in the square see figure 5 the torque can be derived by multiplying the d linked stator flux with the q current minus the q linked stator flux multiplied with the d current and multiply it with the number of pole pairs see equation 21 [5].

$$T_e = \frac{p}{2}(\bar{\Psi}_d \bar{i_q} - \bar{\Psi}_q \bar{i_d}) \tag{21}$$

3.2 Torque calculation using moment of inertia and acceleration

By using the same test sequence but instead measure the acceleration and calculate the moment of inertia on the rotor makes it also possible to calculate the torque [5].

The rotor position is obtained by using the data from the rotor position sensor (θ) that is given by angular frequency. The acceleration of the electrical machine is how much the rotor is changing its speed for every time unit. In order to get the acceleration the angular frequency from the rotor position is derived see equation 22. Since the electrical machine is not ideal not all produced torque will be used to accelerate or brake the machine and therefor another term T_{loss} that represents the friction losses in the rotor has to be added in the equation.

$$\frac{d\omega}{dt} = \frac{\omega(t) - \omega(t-1)}{T_{loss}} \tag{22}$$

By multiplying the moment of inertia with the acceleration and braking for each speed the mechanical torque can be obtained see equation 23 [5]. By

performing this calculation the T_{loss} will disappear since the friction will always point against the angular direction of the rotor.

$$T = J\frac{\overline{\frac{d\omega^{\omega}}{dt} + \frac{d\omega^{-\omega}}{dt}}}{2} \tag{23}$$

The dynamic test method has been proven to be accurate when used with a rotor position sensor, according to [5] the difference in torque measurements between the new test method and traditional test method are less than 0.5%.

For the new test method no additional brake machine is needed, only attaching a flywheel on the rotor of the machine that is being tested may be needed. Because of that, the dynamic test method is much faster than a traditional test method for electrical machines [5]. In the article it is mentioned that the time for performing test of an electrical machine with 100 measurement sequences will only need approximately 2 hours compared with the traditional test method that will use 5 to 6 hours for the same task.

4 Methods for sensorless control

To control a PMSM, three different sensors are usually needed: two current sensors and one rotor position sensor [6]. By using a sensorless control strategy the new test method can also be used for PMSMs that lacks rotor position sensors[10]. According to different research projects the sensorless control methods can be divided in to two groups: fundamental excitation signals and High frequency injection [11] [12]. A tree graph is presented in figure 6 that shows how the different ideas of sensorless control are related to each other.

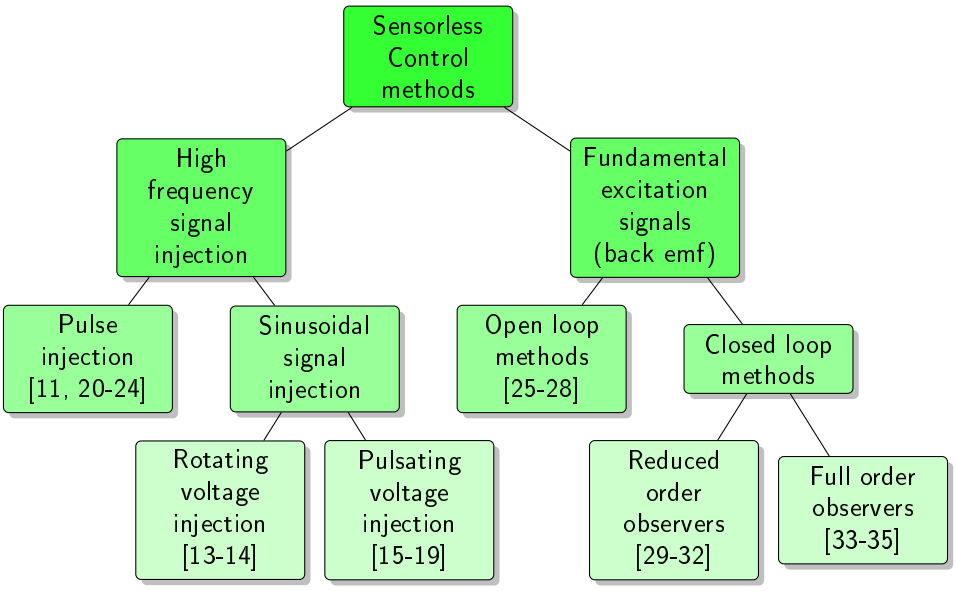

Figure 6: The relationship between different methods for sensorless control.

4.1 High frequency injection sensorless methods

These methods requires an external high frequent signal injection besides current and voltage measurements. The external signal can be injected either in the stationary reference frame ($\alpha\beta$-representation), or in the in the rotating reference frame (dq-representation) [11]. The injected high frequent signal is used to make the saliency of the electrical machine visible for the sensorless rotor position estimation method [11]. Then different methods are used in order to extract information about the error between the estimated rotor position and the actual rotor position [12].

In order to make the estimated rotor position follow the real rotor position an observer is needed [11]. The observer increases or decreases the estimated rotor position and therefor minimizes the rotor position difference between the estimated rotor position and the real rotor position, the observer that is used in one of the high frequency signal injection methods are explained in detail in this chapter.

4.1.1 Rotating voltage injection

Rotating signal injection sensorless methods usually inject a high frequent voltage (sinus and cosine voltages) in both α and β vector. In order to track the rotor position the voltages that are measured are undertaken a heterodyning process. Then the signals are low-pass filtered in order to get rid of the injected signal whereupon the d axis voltage is high pass filtered to get rid of a positive dc current that is not useful for extracting the rotor position. By subtracting the q voltage with the d voltage the difference between the actual rotor position and the estimated rotor position is obtained. Then by adding a PID controller that act as a follower which aims to minimize the difference it is possible to follow the real rotor position [13].

This sensorless control method is presented in the article as completely independent of rotor parameters instead, information about the torque is needed to keep track of the rotor position [13]. It is also claimed that the injected voltage has negligible effect on the performance of the method [13].

The two main components that affect the dynamic performance in this type of sensorless control methods are: the phase delay of the filter, and the responses of the PID controller that is used as a follower.

In [14] a way of improving the dynamic performance of the rotating signal injection sensorless method is presented. The injected signal amplitude increases with increased speed and also a new follower to track the rotor positon is presented. Since the follower uses a minimum of filters in order to improve dynamic performance it instead needs motor parameters. It is claimed that the sensorless control technique is able to handle 250% of the rated torque at standstill.

4.1.2 Pulsating voltage injection

The pulsating voltage injection sensorless methods are quite similar to the rotating voltage injection methods. The main difference is that the high frequency voltage is injected in the rotating reference frame instead of the stationary reference frame.

A completely machine parameter insensitive sensorless control method is presented in [15]. A saturation effect compensation method is presented by taking the use of the rotor design of the machine. The main drawback with this method is that the observer needs to know the torque that is produced by the machine in order to track the rotor position. In [16] the scheme is proven to work with both IPMSM and machines with low saliency SMPMSM.

By injecting both positive and negative sequence pulsating signal it was possible to detect the rotor position more accurate for machines with low saliences without including an observer dependent on machine parameters [17]. By synchronising the injected signal with the PWM inverter it is possible to get rid of lag effects and thereby obtain more accurate rotor position estimation [18].

Overall are both voltage injection methods quite similar in both theory and implementation, however for PMSM it has been found that pulse voltage injection methods are more common in literature [11]. A comparison study was performed

in [19] between two signal injection sensorless methods. It was concluded that it has a small influence on the performance of the sensorless estimation depending on if rotating voltages or pulsating voltages were injected. The only difference that could be observed in this paper is that the error using pulsating voltage injection is slightly smaller than the error using rotating voltage injection.

4.1.3 Pulse injection

In order to obtain the rotor position with this type of method are test voltages injected during short time intervals and the currents from the PMSM are analyzed in order to obtained the rotor position [11]. Notice that this type of sensorless method only works with salient pole PMSMs. Exactly when those test voltages are injected, the voltages and currents over the electrical machine are measured [20]. From the derivative of the currents the phase inductances are identified and since the inductance change depending on the rotor position it is possible to track the rotor position [11].

A popular pulse injection technique is called INdirect Flux detection by On-line Reactance Measurements (INFORM), and follows a special pattern where the inverter is paused and special test voltage vectors are injected. The injections of the test vectors causes some current and torque ripple since the inverter that is feeding the motor have to be paused in order to inject test voltages [21]. This pulse injection method is not using any test voltages to estimate the rotor position but since an alternative PWM has to be used the overall efficency is declined by 15% which may affect the test method [22].

In order to reduce the main disadvantage with pulse injection methods a new pulse injection scheme is introduced in [23]. Normally pulse injections methods are suitable for zero and low speed operation but in order to increase the speed limit a new detection technique is used in [24]. One negative aspect by this method is that in order to calculate the fluxes the value of the q-inductance is needed which means that the method requires a motor parameter.

4.2 Fundamental excitation signals sensorless methods

The methods in this section do not require any signal injections or similar. Instead they obtain the rotor position by voltage and or current measurements from the motor. A drawback these kind of sensorless methods have is that they perform relatively bad when used from stand still and in low speeds.

The sensorless control methods that use fundamental excitation signal can be divided in to two groups of methods, open loop methods and closed loop methods [11].

4.2.1 Open loop methods

The open loop methods do not have any internal correction scheme which makes them work poorly in low speed operations [11]. To be able to make the open loop methods useful they have to be combined with a method for accelerating the

motor at zero and low speeds. That could be by energizing the stator according to a special pattern, by injecting a pulse pattern to the PWM inverter or by using a signal injection sensorless method [6].

In [25] a open loop sensorless control method is presented that can be used in zero and low speed operation. This method does not us back EMF to track the rotor position therefor it is possible to use for low and zero speed operation, instead this method uses the PWM pattern and voltage measurements over all phases in order to determine the rotor position. In order to obtain the rotor position the inductances of the motor have to be known.

The paper "Indirect sensing for rotor flux position of permanent magnet ac motors operating over a wide speed range" [26]presents two ways of measurements in order to obtain the third harmonic voltages, one that was direct measurement on the machines neural network or by measuring on the different phases. The advantage with using the third harmonic voltages for obtaining the rotor position is that it requires a minimum of filtering especially when measuring on the neural network.

By just measuring the voltages and currents from the electrical machine and then performing an integration it is possible to get the back emf flux vector from which the rotor position can be obtained [27]. A rather complicated correctional algorithm is presented in order to prevent errors from the integrations that is performed. Thus this sensorless method has a strong speed limitation which means that this method is not useful for speeds under 1Hz angular velocity.

Another open loop method is based on the electrical steady state circuit in order to obtain the back emf and therefrom obtain the difference between the rotor position and the estimated rotor position [28]. This method does not use any filters hence it will respond very fast to transients. As long as the currents are kept constant it is showed that this method performs accurately.

4.2.2 Closed loop methods

The closed loop methods usually contains some kind of model of the electrical machine that is controlled to be able to correct the rotor position estimation, which makes the closed loop methods less sensitive to motor parameter variations compare to open loop methods. This especially affect the sensorless control in low speed operations [12]. The closed loop methods are divided in to two subgroups depending on the complexity of the correction mechanism: reduced order observer and full order observers [11].

The full order observer usually contains both mechanical and magnetic model of the electrical machine that is being controlled, this means that a lot of motor parameters for the actual motor that is being controlled is needed [11].

The reduced order observer is similar to the full order observer but usually does not contain the mechanical model of the motor, this means that you don't need to know the motor you are controlling as much like in the full order observer case [11].

Reduced order observers

In [29] two different kind of motor model were used: a current model and a voltage model. In order to obtain the rotor position the real voltage or current depending on which motor model that is used are compared with the voltage or current from the model depending on the sign on the difference the rotor position estimation will be increased or decreased.

A more machine parameter insensitive approach for sensorless control is presented in [30]. An Extended Kalman Filter is used as the motor model and the back EMF in order to obtain the rotor position is derived from current measurements. The method was proven to work in both transient state and with detuned motor parameters from standstill to high speed for IPMSMs.

In order to reduce the lag in the rotor position estimation the expected torque is used as a feed forward input in [31], a similar approach is with few variations presented in [32].

Full order observers

The first presented closed loop sensorless control strategy with full order observers is presented in[33]. In this approach, all motor parameters are assumed to be constant. This can cause problem for the rotor position estimation when the motor is saturated. In order to reduce the problem with saturation and changing motor parameter while the motor is running a sensorless control technique is proposed in [34] using a Extended Kalman Filter as the reference model.

The method in [34] is claimed to perform well from high speeds down to 10% of the nominal speed of the motor. In order to make this type of sensorless control usable down to zero speed it needs to be used together with a signal injection method. In [35], is a hybrid sensorless control method presented. In [36]it presents why low speed operation for closed loop methods is performing relatively bad how to overcome those issues with low speed operation, are investigated. It is concluded that when the speed decreases, the back-EMF which includes the rotor position information also decreases, which leads to the signal that contains the rotor position information is drowned in noise created mainly by the inverter and partly by the back-EMF harmonics. In order to make low speed operation possible the bandwidth in the observer is decreased and that leads to side-effects as low robustness in the sensorless control method.

4.2.3 Selection criterions

According to knowledge retrieved from the literature study table 1 is developed, which from certain criterions grades the different sensorless methods. It is important to know that this is a briefly grading for different methods that is valid for the general case and some exceptions may exist but it is decided to insert this figure since it is very good way to inform the reader mainly advantages and drawbacks that each method present.

Table 1: Shows the different properties for the different types of Sensorless rotor position estimation.

	Signal injection	Open Loop	Closed Loop
Low speed operation	High	Low	Low
High speed operation	Low	High	High
Motor parameter dependency	Low	Medium	High

From table 1 it can be seen that the signal injection method for sensorless control can be suitable for use in the test method because its low motor parameter dependency. The reason that does not speak in favor for this sensorless method is that it is only suitable in low speed operation for some current combinations. Also the acceleration and de-acceleration can be to quick for this method. The signal that is injected can also affect how the motor behaves and that can cause this method not being suitable to use for measurements during testing. Instead this method is chosen in order to be able to obtain some motor parameters that later can be used in another sensorless control method. The signal injection method that was chosen is presented in [10] and [37].

Because of the drawbacks with the signal injection method mentioned above another method was also chosen. It is very difficult to find any sensorless control method without external signal injection that does not require any motor parameter. Therefor a sensorless method that requires as little motor parameters as possible have been selected and is from now on refered to as the open loop sensorless method.The open loop method is also chosen because of its simplicity and high speed operation ability. Because of problem with rotor parameter dependency a open loop method that only required one parameter to be estimated is chosen. The voltage injection method [10] [37] and open loop method [38] were both simulated in Matlab Simulink and evaluated, thats is why they are explained in detail below and in this thesis [38].

4.3 Voltage injection method

This section explains more in detail exactly which calculations and blocks that are needed in order to simulate this sensorless method in Matlab Simulink. The overall scheme over the voltage injection sensorless method is presented in figure 7. Layout over model in Simulink

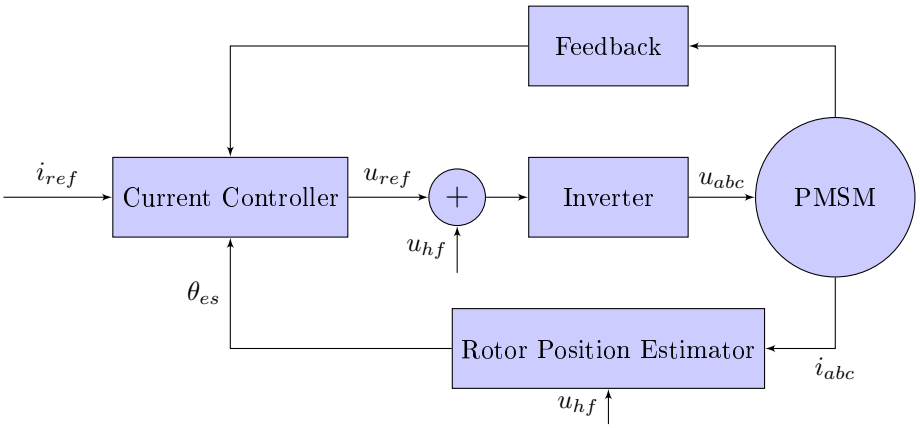

Figure 7: Shows the overall scheme for the signal injection rotor position estimator.

The injected voltage is decided by equation 24 where v_c, is the voltage amplitude of the injected voltage and α is the frequency of the injected voltage. It is important that the frequency of the injected signal is not the same as the frequency from the rotor or the inverter, a typical frequency for the injected signal is between 500 Hz and 2000 Hz [10]. The voltage amplitude should also be selected so a good signal to noise ratio will be achieved [11]. The high frequent voltage can be injected in either α-axis or in β- axis. The voltage is injected after the PI-regulator in the current-control circuit [37].

$$\begin{bmatrix} v_{\alpha h} \\ v_{\beta h} \end{bmatrix} = v_c \begin{bmatrix} cos(\alpha) \\ 0 \end{bmatrix}, where \;\; \alpha = \omega_{ct} + \phi \tag{24}$$

The current response from the electrical machine and the injected voltage are showed in equation 25 and after some calculations it leads to equation 26.

$$\frac{d}{dt}\begin{bmatrix} i_{\alpha h} \\ i_{\beta h} \end{bmatrix} = \begin{bmatrix} \frac{1}{L_p} + \frac{1}{L_n}\cos(2\theta_r + \theta_m) & \frac{1}{L_n}\sin((2\theta_r + \theta_m) \\ \frac{1}{L_n} = \sin(2\theta_r + \theta_m) & \frac{1}{L_p} - \frac{1}{L_n}\cos(2\theta_r + \theta_m) \end{bmatrix} \cdot V_c \begin{bmatrix} cos(\alpha) \\ 0 \end{bmatrix} \tag{25}$$

$$\begin{bmatrix} i_{\alpha h} \\ i_{\beta h} \end{bmatrix} = \begin{bmatrix} I_p + I_n\cos(2\theta_r + \theta_m) \\ I_n\sin(2\theta_r + \theta_m) \end{bmatrix} \cdot V_c \begin{bmatrix} cos(\alpha) \\ 0 \end{bmatrix}, I_n = \frac{V_c}{\omega_c L_p}, I_p = \frac{V_c}{\omega_c L_n} \tag{26}$$

The currents in equation 26 are processed with a method called heterodyning which means that the signal is multiplied with $2\sin(\alpha)$. After that the signal is Low pass filtered and the result can be seen in equation 27. The injected high signal from equation 24 is now gone and now the signal contains a DC part, a cosine signal that contains the rotor position information in the α frame and a sinus with rotor information in the β frame.

$$\begin{bmatrix} |i_{\alpha h}| \\ |i_{\beta h}| \end{bmatrix} = LPF\left(\begin{bmatrix} i_{\alpha h} \\ i_{\beta h} \end{bmatrix} \cdot 2\sin(\alpha) \right) = \begin{bmatrix} I_p + I_n \cos(2\theta_r + \theta_m) \\ I_n \sin(2\theta_r + \theta_m) \end{bmatrix} \tag{27}$$

After this, the α part is multiplied with $\cos(\theta_r)$ and the β part is multiplied with $\sin(\theta_r)$. Then θ_r comes from the feedback in the phase locked loop, see equation 28.

$$\begin{bmatrix} |i_{\alpha h}| \\ |i_{\beta h}| \end{bmatrix} \cdot \begin{bmatrix} \sin(2\theta_e) \\ \cos(2\theta_e) \end{bmatrix} \tag{28}$$

In equation 29 the current from the first and second row in equation 28 is subtracted to eachother, and that leads to a single sinus function as can be that contains the rotor position error . It is towards this error the phase locked loop is working.

$$|i_{\alpha h}| \sin(2\theta_e) - |i_{\beta h}| \cos(2\theta_e) = \sin(2(\theta_r - \theta_e)) \approx I_n 2(\theta_r - \theta_e) \tag{29}$$

The approximation in equation 29 is only valid for small errors, so the assumption only works when the phase locked loop is accurately tuned. The goal of the phase locked loop is to increase the rotor position θ_e so that θ_r-θ_e is as close to zero as possible, which means that the rotor position estimation is closely following the real rotor position. The overall scheme of the signal injection based rotor position estimator that is simulated in Matlab Simulink is shown below in figure 8.

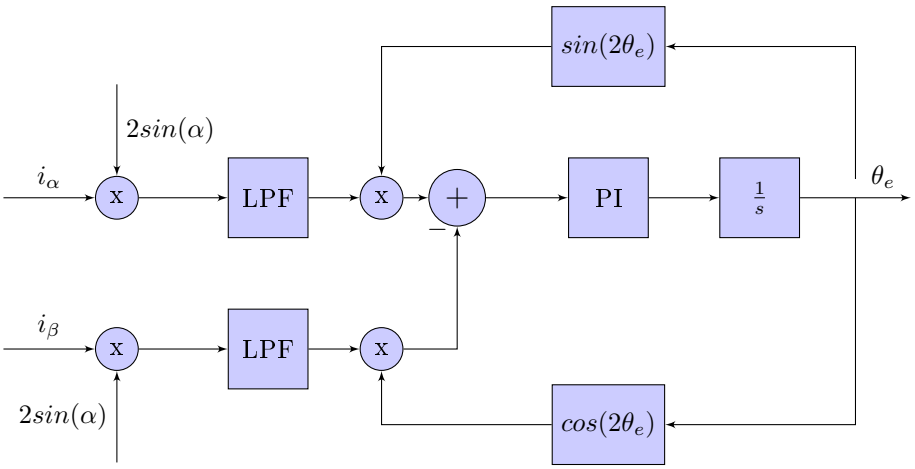

Figure 8: Shows the overall scheme for the signal injection rotor position estimator.

4.4 Open Loop

The overall layout of the set up with motor, inverter, controller and Open Loop rotor position estimator is shown in figure 9.

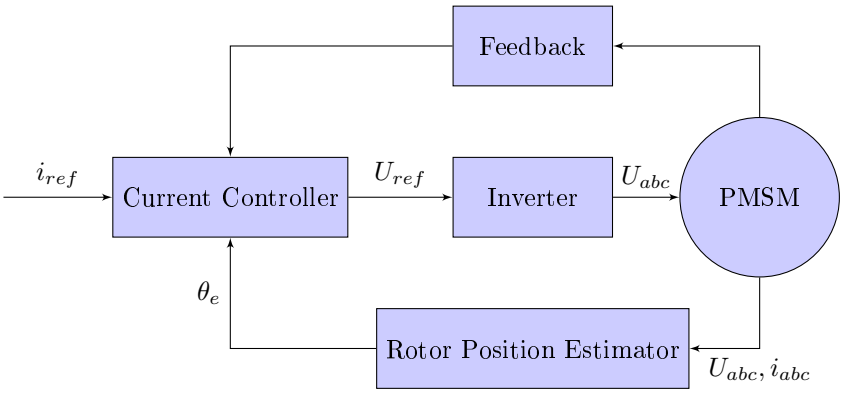

Figure 9: Shows the overall scheme for the Open Loop rotor position estimator.

The rotor position estimator block from figure 9 is in more detail described by figure 10 below.

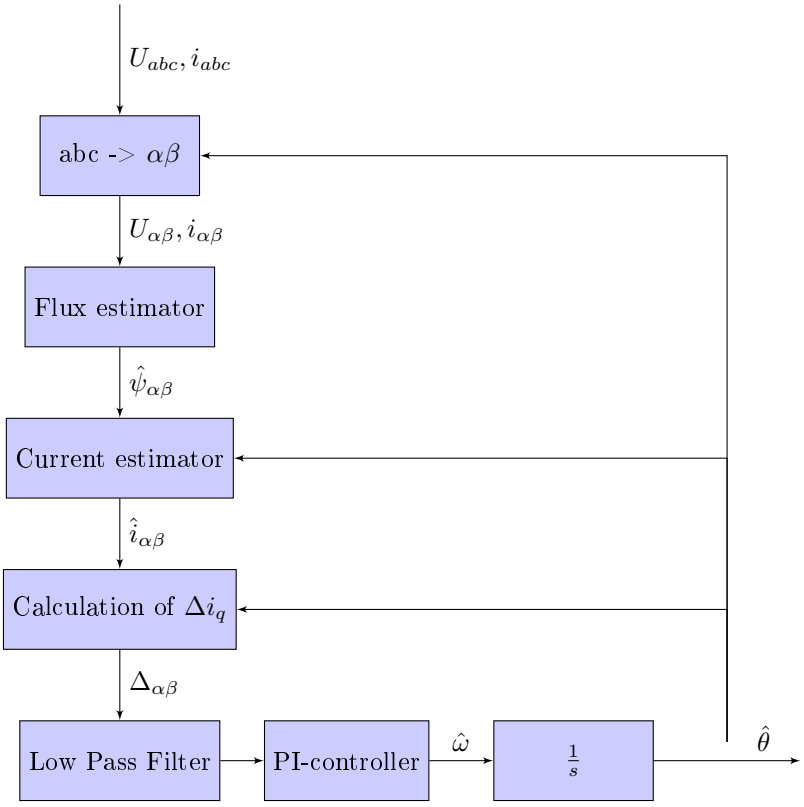

Figure 10: Shows the calculation blocks for the Open Loop rotor position estimator.

Below every calculation from figure 10 needed for this sensorless rotor position estimator are presented. The source for this method is [38]. First the flux is

estimated by integrating the voltage subtracted with the current and resistance according to equation 30.

$$\hat{\psi}_{\alpha\beta} = \int (V_{\alpha\beta} - Rs_{\alpha\beta})\mathrm{d}t \tag{30}$$

Then the currents are estimated by following calculations in equation 31, where $\hat{\theta}$ is the estimated rotor position that is estimated by the method.

$$i_\alpha = \frac{1}{L}[\hat{\psi}_\alpha - \psi_m cos(\hat{\theta}] \qquad i_\beta = \frac{1}{L}[\hat{\psi}_\beta - \psi_m cos(\hat{\theta}] \tag{31}$$

The difference between the estimated and measured currents are calculated in equation 32.

$$\Delta i_{\alpha\beta} = i_{\alpha\beta} - \hat{i}_{\alpha\beta} \tag{32}$$

Then the currents from equation 32 is transformed from $\alpha\beta$ to dq-frames according to equation 33.

$$\Delta i_q = -\Delta i_\alpha sin(\hat{\theta}) + \Delta i_\beta cos(\hat{\theta}) \tag{33}$$

Δi_q is the signal that goes to the PI controller that works to minimize the error by increasing Δi_q, therefor it can be said that the PI-controller is tracking the speed. The signal from the PI-controller is then integrated to get the rotor position.

5 Simulation model

This section has been created to inform the reader in detail about how the model for validating the sensorless control strategy with the test method is created. Figure 11 shows the simulation model. It contains the following blocks: reference currents, signal injection, current controler, PMSM model, simulation data and rotor position estimator.

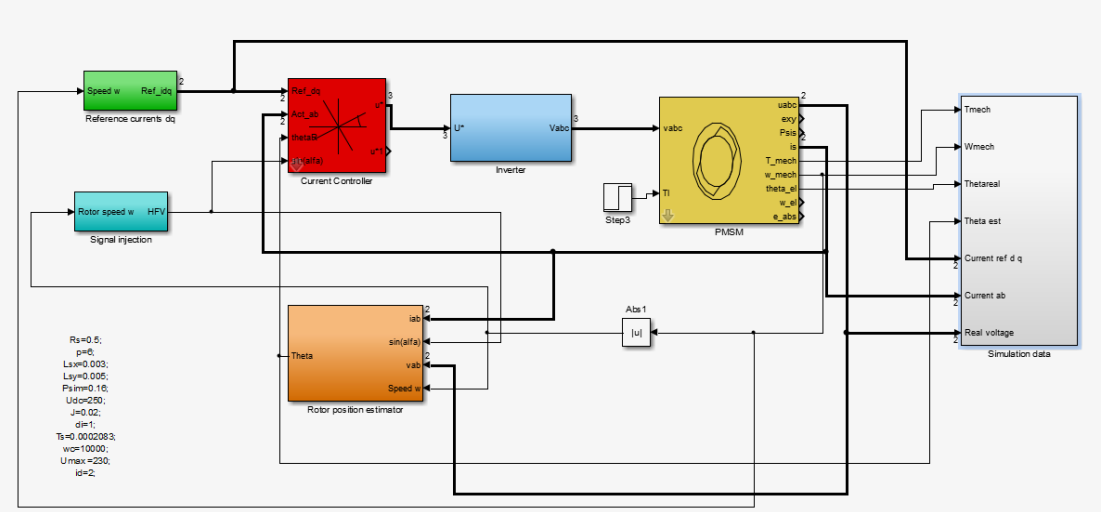

Figure 11: Shows a overview scheme of the simulation model that was used.

5.1 Model of PMSM

In the beginning of the project the methods are simulated together with a linear model of an PMSM. In reality the PMSM does not act linnear because of saturations effects. This means that the PMSM for example does not necessarily create twice as much torque when the current is doubled. To create a more realistic model of the PMSM flux maps that are obtained from a real electrical machine in this PhD thesis [39] are used. Since the flux maps are retrived from measurement with the new dynamic breaking test method of a real PMSM, it can be assumed that the model of the PMSM acts like the real PMSM in terms of losses and saturation.

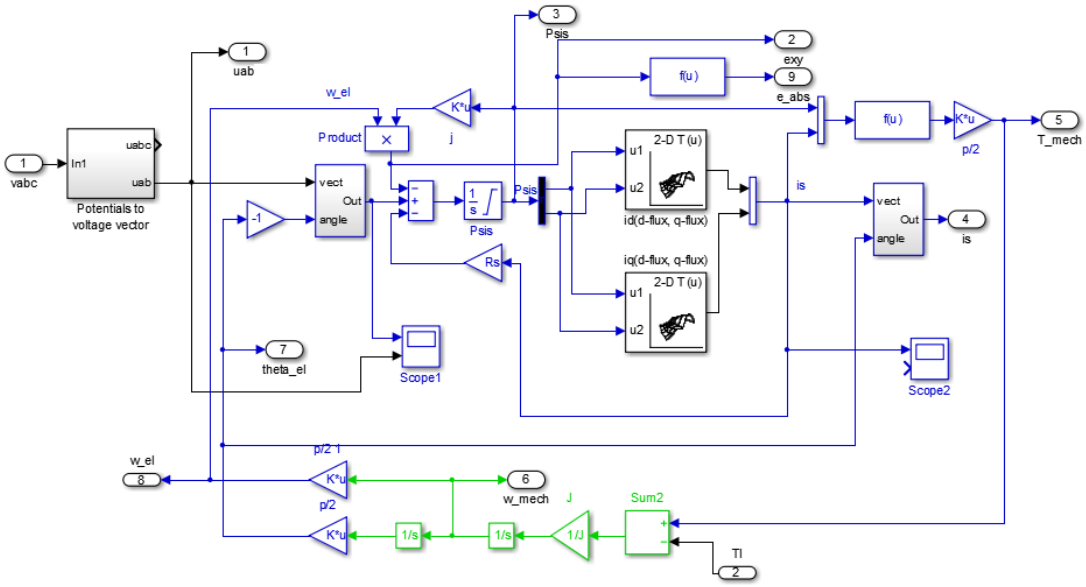

Figure 12: Shows the model of the PMSM that is used in the simulations. The model is originally made by Mats Alaküla and are just slightly modified in order to use the flux maps.

As can be seen in figure 12 the model of the PMSM that is used first transforms the incoming voltages to the rotating reference frame (dq). Then by performing an integration of the incoming voltages minus the resistance times the currents and minus the speed times the inverse fluxes the fluxes are calculated as can be seen in equation 34. Then depending on the flux values the currents was obtained from the currents maps that are derived from the flux maps.

$$\begin{bmatrix}\Psi_d \\ \Psi_q\end{bmatrix} = \int \begin{bmatrix}v_d \\ v_q\end{bmatrix} - R_s \begin{bmatrix}i_d \\ i_q\end{bmatrix} - \omega_{el} \begin{bmatrix}-\Psi_d \\ \Psi_q\end{bmatrix} \mathrm{d}t \tag{34}$$

The torque from the PMSM model is calculated according to formula 35 below where p is the number of poles for the machine.

$$\Psi_d \cdot i_q - \Psi_q \cdot i_d = T_{mech}, T_{el} = T_{mech} \cdot \frac{p}{2} \tag{35}$$

The rotor speed is calculated by integrating the torque minus the breaking power from an external object T_i see equation 36, where J is the mass of the rotor.

$$\omega_{mech} = \int (T_{mech} - T_i) \cdot \frac{1}{J} \mathrm{d}t, \; \omega_{el} = \omega_{mech} \cdot \frac{p}{2} \tag{36}$$

5.2 Inverter

The inverter contained 3 switches that feed the PMSM-model with different positive and negative DC-currents. The switch contained a triangular wave

with the frequency of 10kHz. The inverter are feed by Vdc and -Vdc which has the following voltage levels 150V and -150V. The simulation model of the inverter that is used can be seen in figure 13.

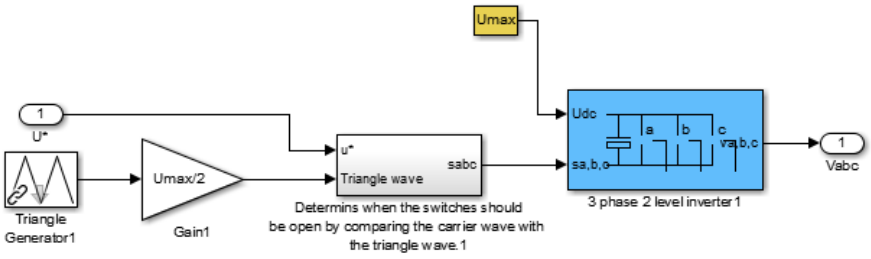

Figure 13: Shows the inverter that was used in the simulations.

5.3 PI current controller

The PI-controller that is used in the simulations is taken from one of the home assignments in the power electronics course in IEA LTH. The high voltage injection is performed just after the current controller as can be seen in figure 14.

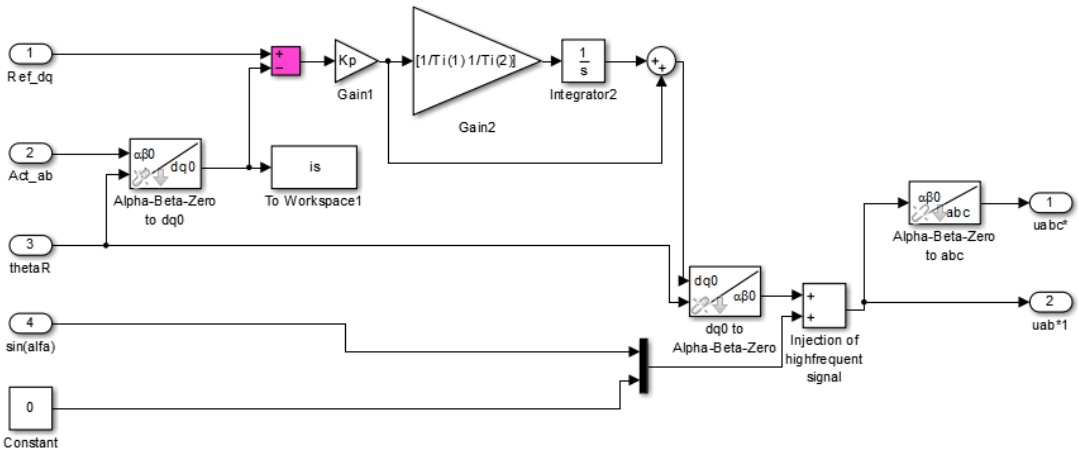

Figure 14: Shows the current controller block.

5.4 Current provider

The current reference provider that can be seen in figure 15, is created to give the correct reference currents to the current controller according to the test

method for PMSMs. The current provider also make it possible to use two different current combinations that switched depending on the rotor speed, this function is useful when using the pulsating injection method to accelerate the PMSM and then let the open loop method take over. The relay signal had the value of 2 before and after the measurements for the test method is performed.

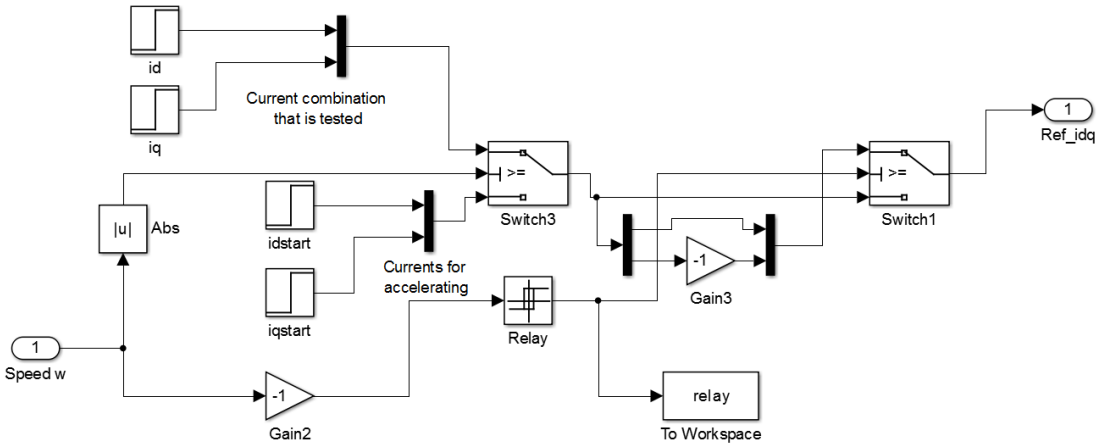

Figure 15: Shows the block for reference currents.

5.5 Sensorless methods

Since this master project contained two different sensorless rotor position estimation methods both of them are implemented in Simulink. To change which sensorless method that is used during simulations, a switch is set up as can be seen in figure 16.

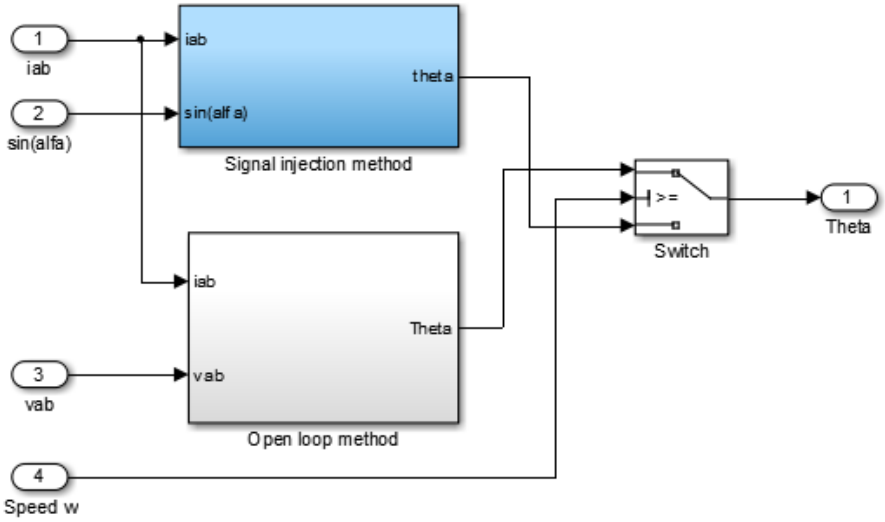

Figure 16: Shows the two sensorless methods block and a switch that change metod depending on the rotor speed.

The block for decoding the current response from the PMSM followed the description that has been given in earlier chapters are presented in figure 17. An issue with this method is to find a proper filter to get rid of the high frequent signal. Since the observer needed to get the rotor position with as small phase lag as possible a Bartlett Hanning filter design with the cut frequence of 700Hz was selected. The PI-controllers gain are selected from the article that presented the sensorless control strategy with the values of $k_p = 500$ and $k_i = 1000$ [37].

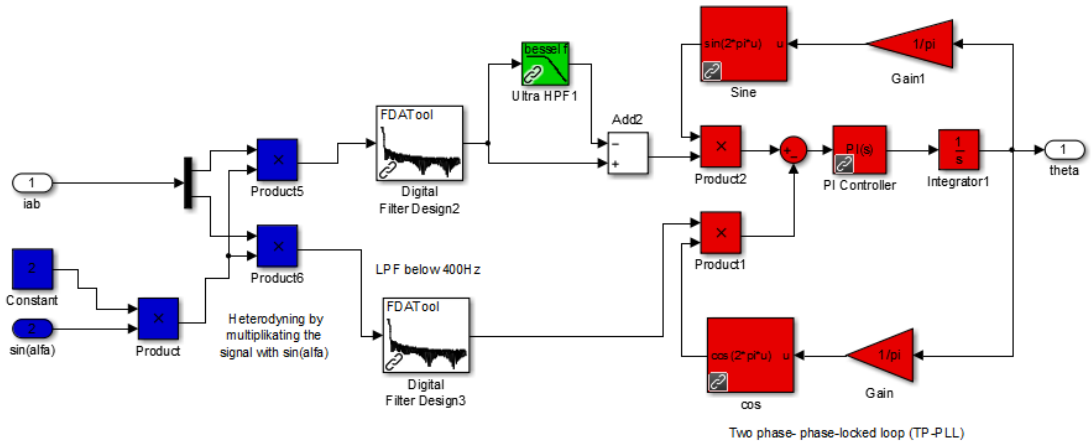

Figure 17: Shows the blocks that was used for decoding the signals from the PMSM in the signal injection method.

The open loop method is easy to build since the method is well described in [38] and the Simulink implementation is shown in figure 18. The gains of the PI-controler are found by testing different PI gain values and compare how well the sensorless method is following the rotor position. It is concluded that the k_p should be 15 and k_i should be 584.

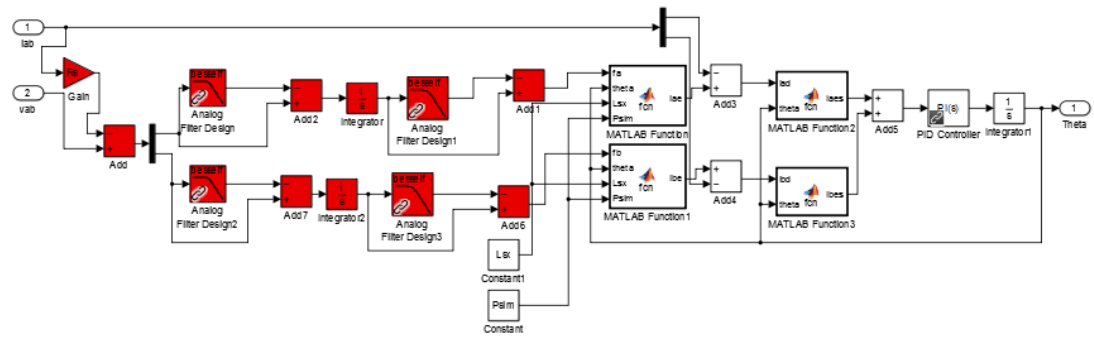

Figure 18: Shows the blocks that was used for the open loop method.

5.6 Testing

To evaluate the different sensorless methods that is presented in this project a simple script in Matlab is written so that all the results are created in a similar way. The script runs the simulation for different currents injected to the PMSM in the dq frame and the result is then saved in a matrix where the the x and y

axis represents the d and q -currents. To illustrate the results the result matrixs is plotted by a 3d plot function called surface in Matlab.

In order to test the different sensorless methods flux maps are taken from another project and used in this thesis [39]. In that thesis the dynamic braking method is used with the following current combinations i_d = 0:-70 A and i_q = 10:70 A, that is also why those current combinations are used in order to test the sensorless methods.

The measurements for the open loop sensorless method the results is only recorded when the motor has reached a speed of minimum 60 rad/s. The reason for this is because the sensorless method does not work at all for speeds under 60 rad/s.

6 Results

This section presents the results from the different rotor position estimation methods used with the dynamic test method.

First are the fluxes that has been used for simulating the motor in Matlab Simulink presented. The fluxes have been created in [39] and have been obtained by using the new dynamic test method together with a rotor position sensor.

In figure 19 it can be seen that the d-flux depends on the amount of the d-current the PMSM is feed with. Just as it is described in equation 7 earlier. In figure 20 the q-flux is presented it can be seen that it depends on how much q-current the PMSM is feed with and that is correlating to how the q-flux is described in equation 8.

The results that is important to get is the d-flux and q-flux because from that information the torque can be calculated. It is the same parameters that the new test method needs to obtain.

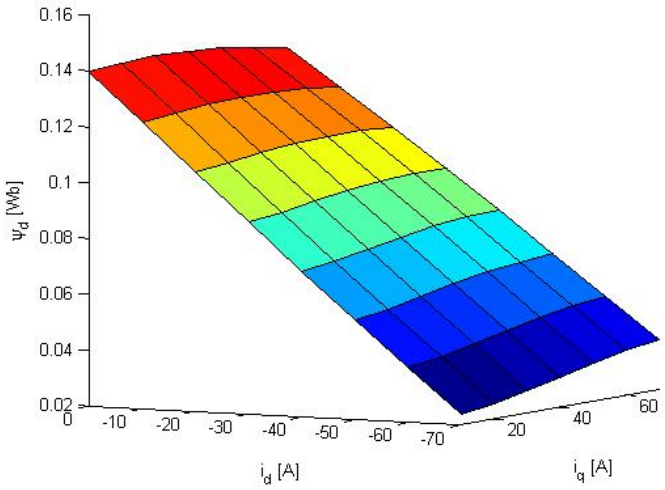

Figure 19: Ψ_d under different current combinations that have been found via the dynamic testing method during sensored mode of the PMSM [39].

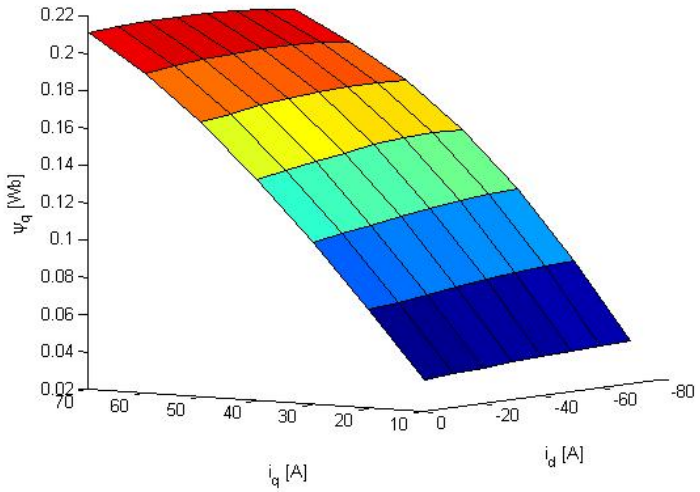

Figure 20: Ψ_q under different current combinations that have been found via the dynamic testing method during sensored mode of the PMSM [39].

6.1 Pulsating injection rotor position estimator

The main purpose for this method in this master project is to obtain the motor parameters that is needed for the open loop sensorless method. That is because of the pulsating injection can create saturations effects on the PMSM and that makes the values obtained by this method not reliable for the new test method. So the signal injection methods main purpose is to obtain the ψ_{pm} and ψ_d values from which the L_d and ψ_{pm} can be obtained. Those are the motor parameters used by the open loop method.

A full cycle for one current combination in this method showing speed, currents, rotor position error and torque is presented in figure 21. In figure 22 a cycle for another current combination is presented, it can be seen that the rotor position tracking in this cycle is not very successful.

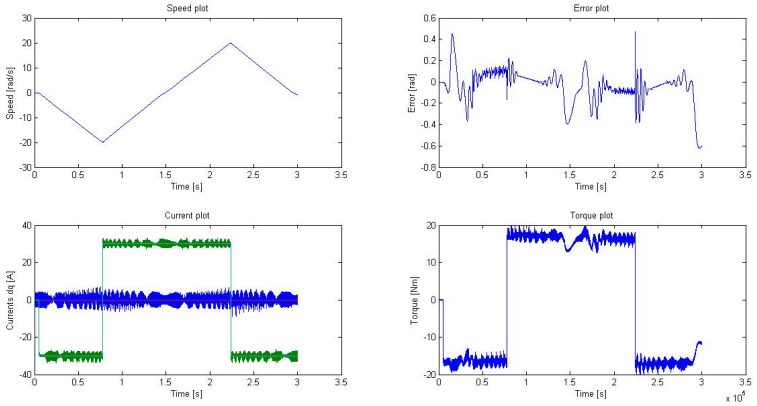

Figure 21: Shows a test sequence with the pulsating injection method.

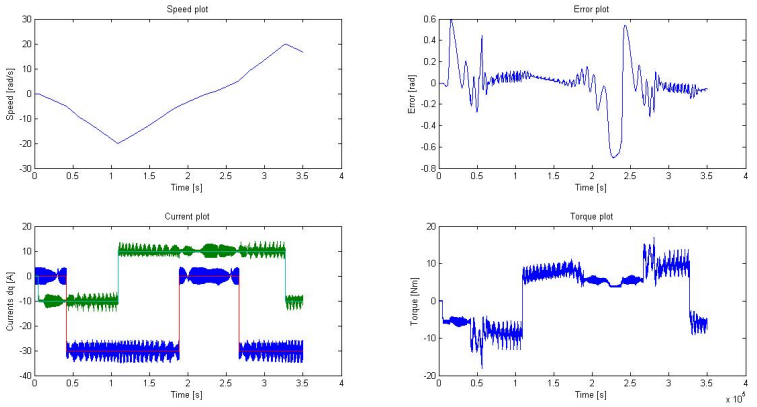

Figure 22: Shows a test sequence were the pulsating injection method is not performing very well.

A problem that was found with the signal injection method is that it could only track the rotor position for a few current combinations. In order to make the signal injection method tracking the rotor position for more current combinations the rotor inertia was increased. It is shown in figure 23 that increasing rotor inertia does not help this method to keep track of the rotor position when increasing the field weakening current i_d.

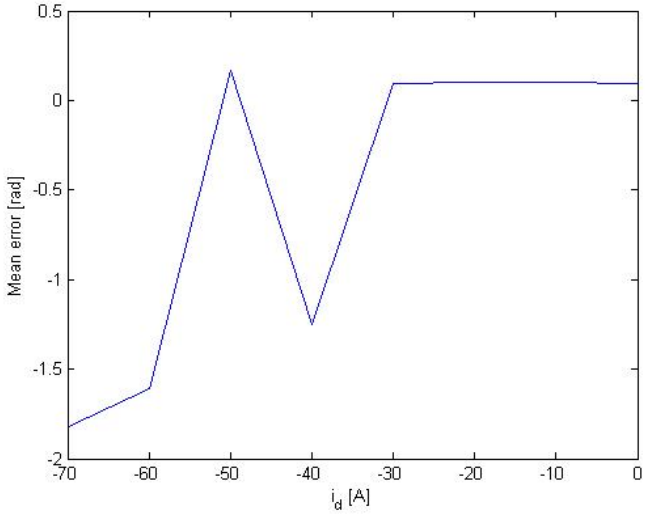

Figure 23: How the mean error variates depending on the i_d current. The rotor inertia was increased when the current increased. In this figure the i_q current was kept to 10 A.

In figure 24 it is shown that by increasing the rotor inertia the method could track the rotor position for the full spectra of i_q currents. This is not very helpful though the ψ_d and ψ_{pm} depends on the i_d current according to equation 7.

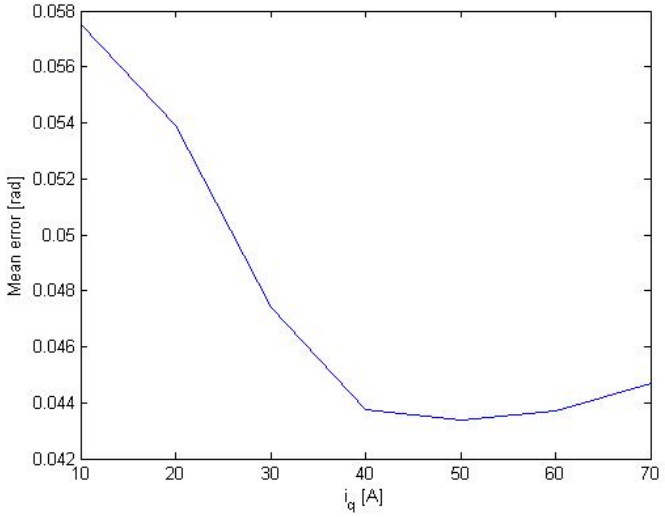

Figure 24: Variation of the mean error varies depending on the i_q current. The rotor inertia increases when the current increases.

In order to see if the pulsating injection method lost track of the rotor position due to saturation effects the method is tested for a PMSM model were the fluxes increases linear. It can be seen in figure 25 that the signal injection sensorless control method can keep track of the rotor position for all current combinations. In this test the rotor inertia was increased when i_q is increased in order to not accelerate too fast so that the filters in the control method will lag too much and the method will lose track of the rotor position.

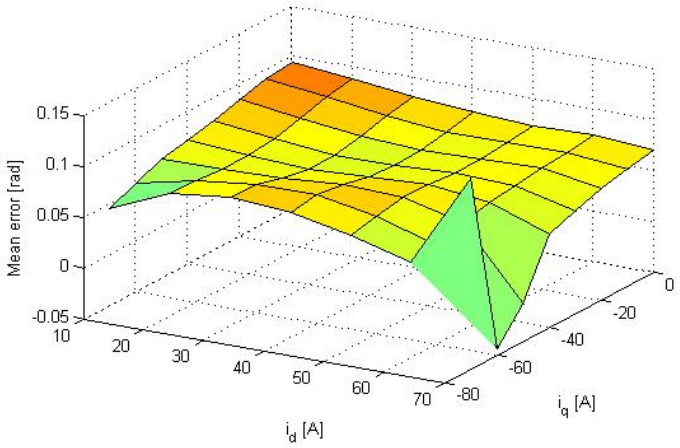

Figure 25: The accuracy of the rotor position estimation when the PMSM model is behaving linear (no saturation effects).

In order to make it possible to use the ψ_d values usable some extrapolation is needed because the sensorless voltage injection method has problem with handling the saturation effects in the windings. Below in table 2 are the ψ_d for different i_d currents for which it is possible for the pulsating injection method to keep track of the rotor position is presented. When the field weakening i_d current is getting larger it is harder for the sensorless method to keep track of the rotor position it is found during the thesis work that by increasing the i_q current it could be possible to track the rotor position for larger field weakening currents i_d to some extent. The real values that are presented in table 2 are the values that has been obtained in [39].

Table 2: Obtained values for ψ_d, ψ_d and torque that has been obtained by the test method together with the pulsating signal injection method.

i_d	i_q	T	$est\psi_d$	$real\psi_d$	$diff\psi_d$	$est\psi_q$
0	10	5.36	0.1354	0.1398	0.0044	0.0276
-10	10	5.92	0.1182	0.1228	-0.0100	0.0302
-20	10	7.14	0.1122	0.1058	0.0064	0.0311
-30	30	23.42	0.1019	0.0920	0.0099	0.0950
-40	30	25.33	0.0858	0.0758	0.01	0.0950

The result from the extrapolation of ψ_d is showed in figure 26, the Matlab built in function polyfit was used.

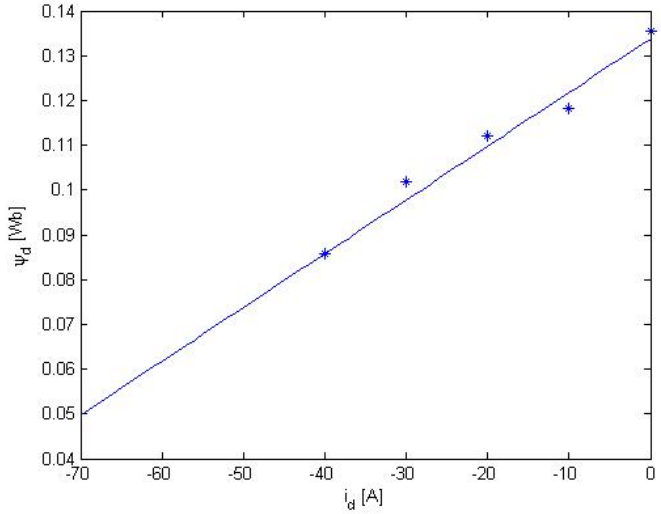

Figure 26: The extrapolation of ψ_d.

In table 3 the extrapolation values of ψ_d are presented and they are also compared with the values for the PMSM that is obtained in [39]. It can be seen that the extrapolation gets worse the further away from the obtained values it goes. That depends on that the ψ_d behaves linearly up to a certain value of the i_d current and when the current is increase further it will occur some saturation effects and the ψ_d will not behave linearly anymore. The question for the future is now if the open loop sensorless method will work for the obtained motor parameter when i_d is -70.

Table 3: The Q-flux estimated by extrapolate the values obtained by the new test method together with the signal injection sensorless control.

i_d	est. ψ_d	real ψ_d	diff. ψ_d
-70	0.0498	0.0307	0.0191
-60	0.0618	0.0463	0.0155
-50	0.0738	0.0618	0.0120
-40	0.0858	0.0774	0.0084
-30	0.0978	0.0929	0.0049
-20	0.1098	0.1085	0.0013
-10	0.1218	0.1240	-0.0022
0	0.1338	0.1393	-0.0055

6.2 Open Loop rotor position estimator

First a sensitivity analysis is performed on this sensorless method to be able to see how sensitive this method is to motor parameters deviations. In figure 27 it is shown how the error depends on how accurate the motor parameters are for the open loop method. It can be concluded that the method is not very sensitive to the ψ_{pm} parameter and that its performance mainly depends on

how accurate the L_d values is. Notice that the motor parameters are presented as absolute values so 1 equals to exactly the value of the motor parameter and 0.7 equals to 0.7 of the exact motor parameter and so on.

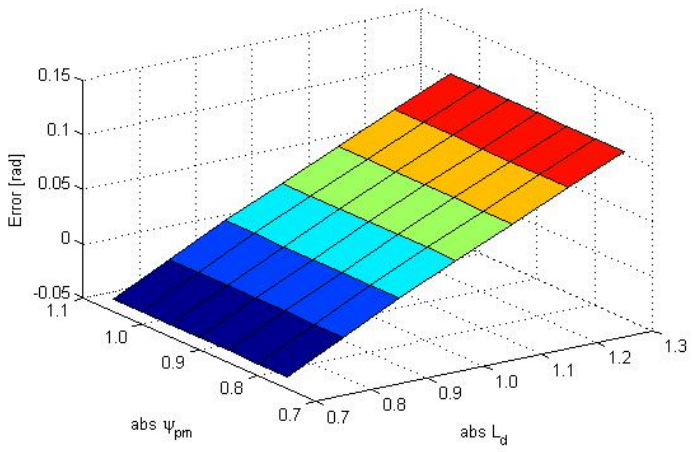

Figure 27: Shows a graph over how the mean error variates for the rotor position by changing the motor parameters that is not able to measure without the test method.

When the PMSM is exposed to for example a current step it always takes some time until the sensorless method has stabilized itself for tracking the rotor position. In figure 28 it is shown the time it takes for the open loop method to stabilize itself. It can be seen from the figure that it takes approximate 0.08 seconds for the rotor position estimator to stabilize, this is used in order to know on which values the test method can be used because if the rotor position tracking is not good the values obtained will not be accurate.

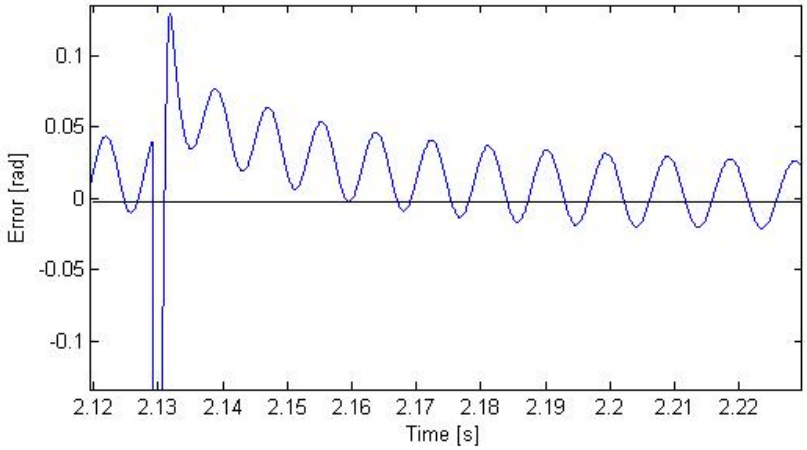

Figure 28: How fast the rotor position estimation stabilize itself after a step response.

Because of the bad performance of the open loop method in low speeds the sensorless injection method has to be used when the speed is low in the test cycle, see figure 29. When the speed is low and the pulsating injection method is used during the test cycle the current combination that is feed to the PMSM is changed to a current combination the signal injection method can track the rotor position in.

Figure 29: A test cycle for a current combination.

Below are the results from the test method used together with the open loop method that uses the motor parameters obtained and extrapolated from the pulsating signal injection method. The ψ_d values that are shown in figure 30 behaves like it should be according to the theory since the amount of ψ_d mostly depends on the i_d current see equation 7.

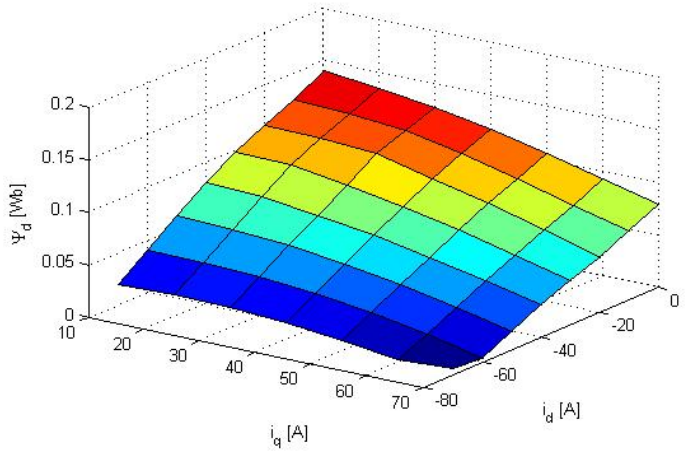

Figure 30: ψ_d produced by the PMSM obtained by the new test method together with the open loop sensorless control.

In figure 31 is the ψ_q values that has been obtained presented, also here it can be concluded that the ψ_q mainly depends on the i_q current just according to equation 8.

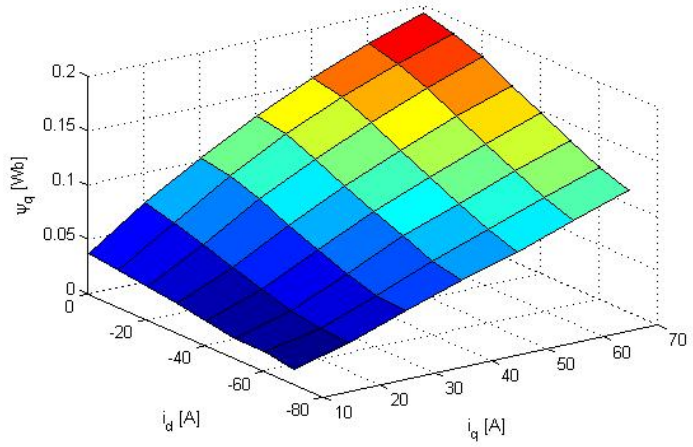

Figure 31: ψ_q produced by the PMSM obtained by the new test method together with the open loop sensorless control.

According to the new test method also the torque can be obtained. The new test method uses the fluxes in order to obtain the torque. The torque produced in different current combinations are presented in figure 32.

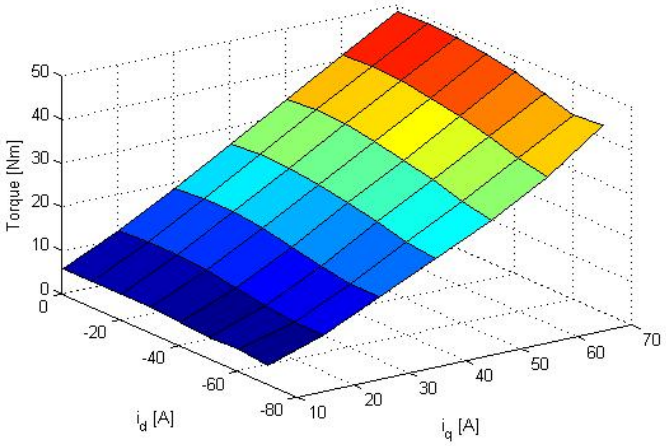

Figure 32: The torque produced by the motor obtained by the new test method together with the open loop sensorless control.

In order to see how accurate the new test method is together with sensorless control the obtained values was compared with the real values that has been obtained with the new test method in sensored mode from [39]. The differences in the ψ_d is presented in figure 33, it can be seen that the accuracy of becomes worse when the i_q currents is increased.

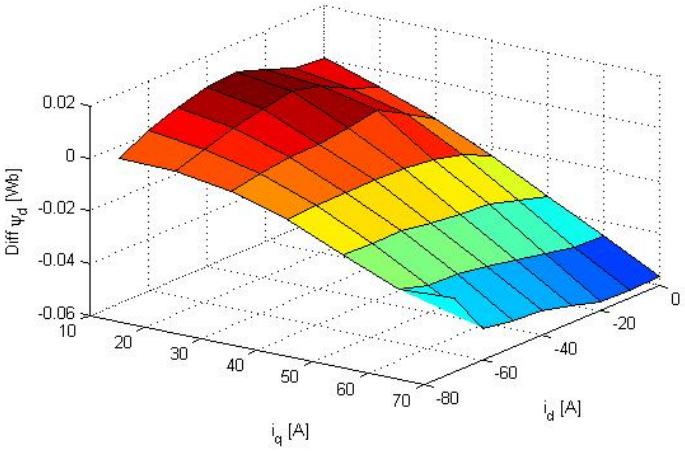

Figure 33: The difference between the obtained ψ_d and the real ψ_d values.

In figure 34 it is showed that the accuracy for the test method together with sensorless control gets worse both when the i_q and i_d is increased.

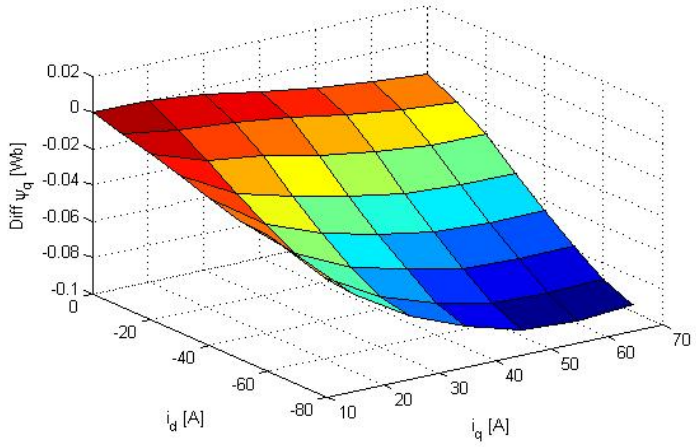

Figure 34: The difference between the obtained ψ_q and the real ψ_q values.

The performance on the dynamic sensorless test method is worse at big i_d and i_q currents. An explanation for that could be that the obtaining of motor parameters with the voltage injection sensorless method is worse at large i_d currents and that makes the open loop control method perform not as accurate. Another reason could be that when the i_d current is high and the i_q current is high the acceleration of the PMSM also becomes high which then challenging the dynamic performance of the sensorless control. A way to ease the dynamic stress on the sensorless control is to increase the rotor inertia by adding a flywheel on the rotor shaft.

6.2.1 Motor parameters obtained by a second iteration

In order to investigate if the performance of the test method together with sensorless control increases with more accurate motor parameters the flux values that are obtained just above in this thesis are used as motor parameters in the open loop method. Below are the results from the test method is used together with the open loop method with motor parameters obtained from the last iteration. In figure 35 and 36 are the d and q flux presented for different current combinations.

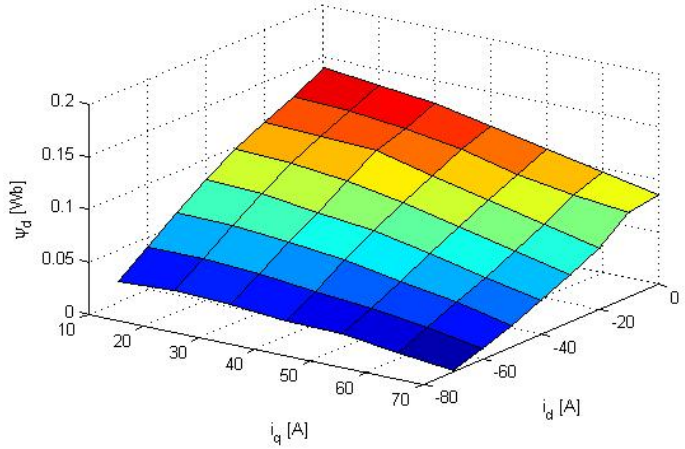

Figure 35: D-flux produced by the PMSM obtained by the new test method together with the open loop sensorless control during the second iteration.

It can be seen that the fluxes behaves according to the theory see equation 7 and 8.

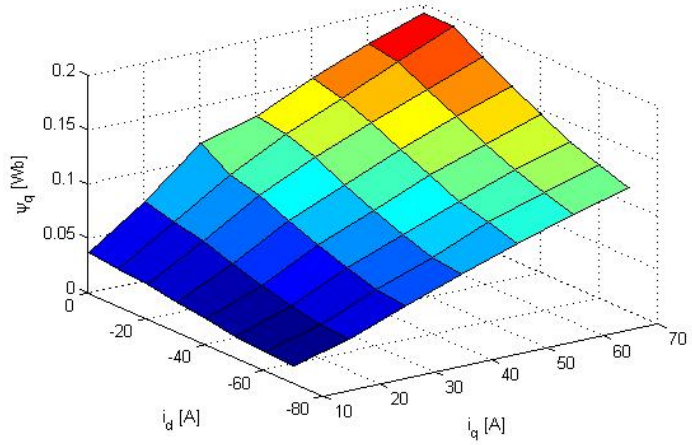

Figure 36: Q-flux produced by the PMSM obtained by the new test method together with the open loop sensorless control during the second iteration for motor parameter identification.

The torque map that is obtained is presented in figure 37, and it can be seen that the produced torque mainly follows the amount of i_q that is feed to the PMSM.

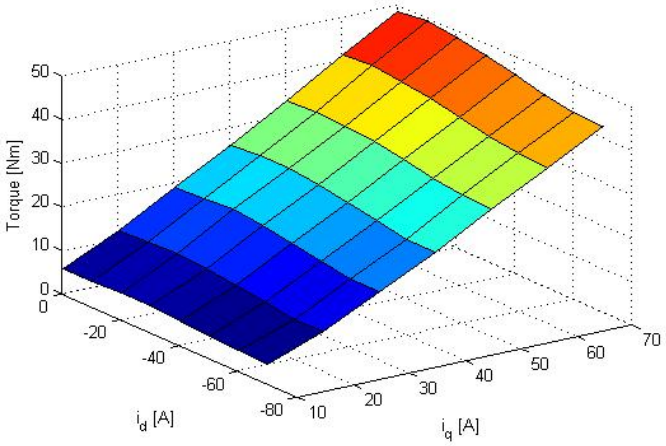

Figure 37: The torque produced by the motor obtained by the new test method together with the open loop sensorless control during the second iteration.

When the obtained fluxes are compared with the real fluxes it can be seen that the more accurate motor parameters did not improve the results significantly. In figure 38 it is shown that the difference increases with increased i_q current.

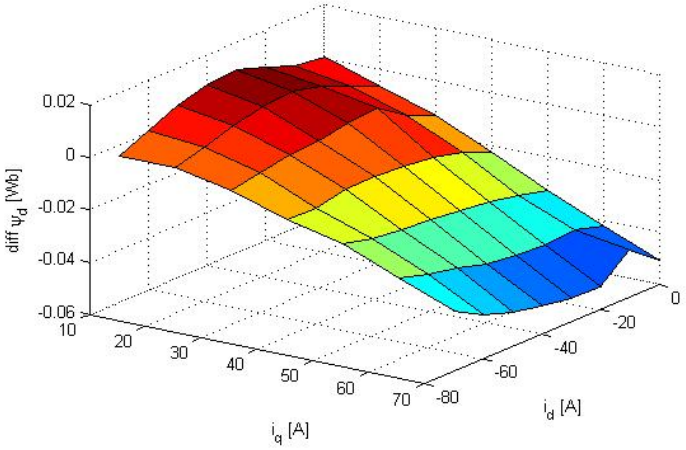

Figure 38: Shows a graph over how the mean error variates for the rotor position by changing the motor parameters that is not able to measure without the test method.

It can be seen in figure 39 that the difference between the obtained and real ψ_q is not decreased compared with the last run presented. The difference is still increasing with increased i_d and i_q currents.

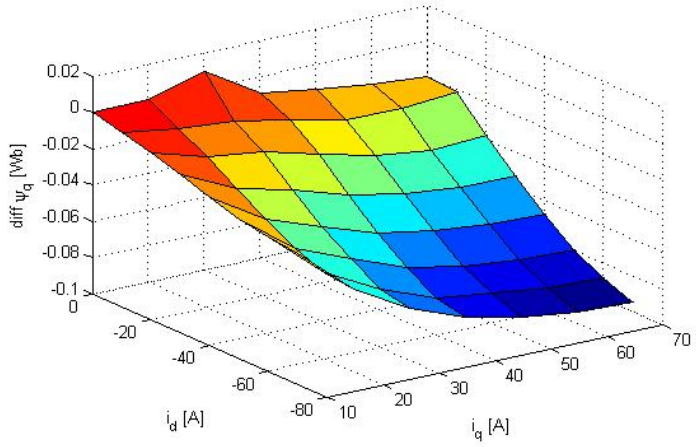

Figure 39: Shows a graph over how the mean error variates for the rotor position by changing the motor parameters that is not able to measure without the test method.

6.2.2 Compensation

In the paper about the open loop method that was used [38] a compensation method was used in order to get a more accurate rotor position tracking. The compensation method is by simply just adding a value to the rotor position estimation signal. A simple compensation was tried to see if any improvement of the results was reached.

Below in figure 40 is the ψ_d presented and it is again following the theory that it is mostly depending on the field weakening current i_d.

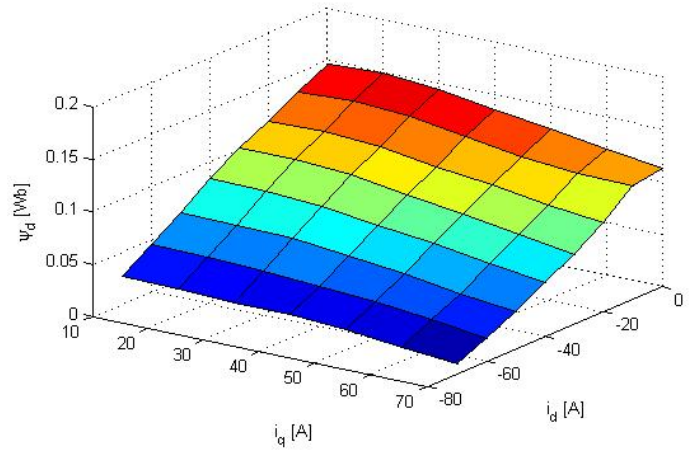

Figure 40: D-flux produced by the PMSM obtained by the new test method together with the open loop sensorless control with open loop compensation.

In figure 41 is the ψ_q presented and again it is behaving like it is explained in equation 8, that the flux is increased when i_q current is increased.

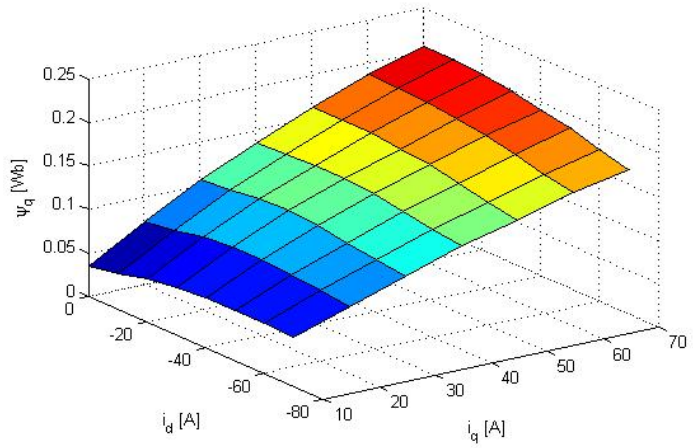

Figure 41: Q-flux produced by the PMSM obtained by the new test method together with the open loop sensorless control with open loop compensation.

Below in figure 42 is the torque shown for the PMSM and again it is behaving like it should, it mostly depends on the i_q current.

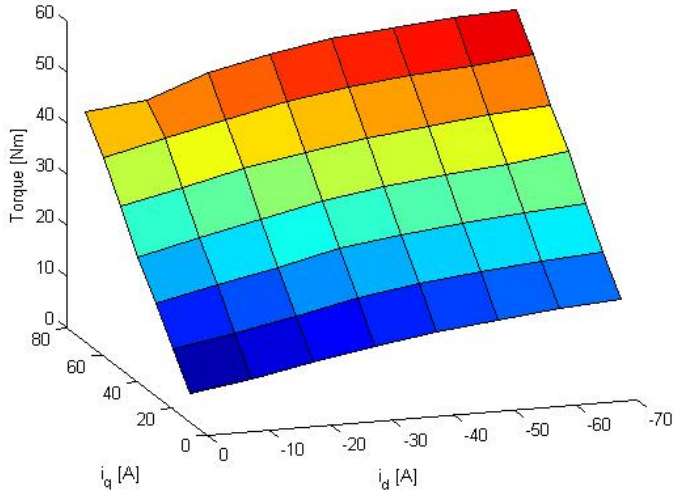

Figure 42: The torque produced by the motor obtained by the new test method together with the open loop sensorless control with open loop compensation.

It can be seen in figure 43 that the difference between the real and obtained ψ_d has been decreased, the compensation had a positive effect on the result. It

could be seen that the largest difference between the methods are around 0.03 Wb compare with 0.05 Wb without compensation.

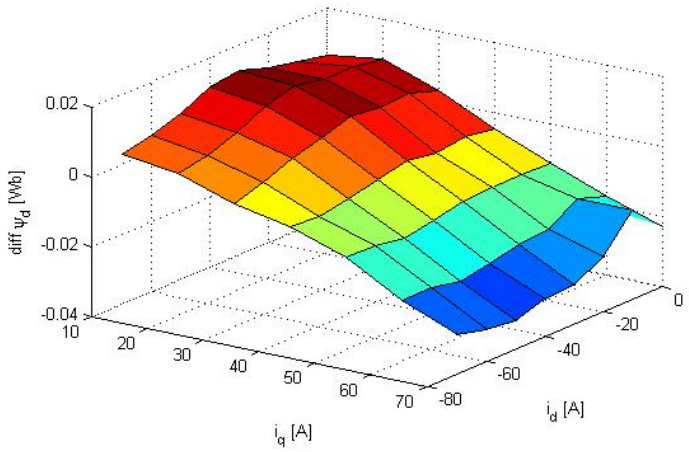

Figure 43: The difference between the real ψ_d and the obtained ψ_d when using the new test method together with open loop sensorless control with compensation.

In figure 44 is the difference between the obtained ψ_q and the real ψ_q presented. Also here it can be seen that the maximum error has decreased from 0.09 to 0.04 Wb due to the compensation of the sensorless open loop method.

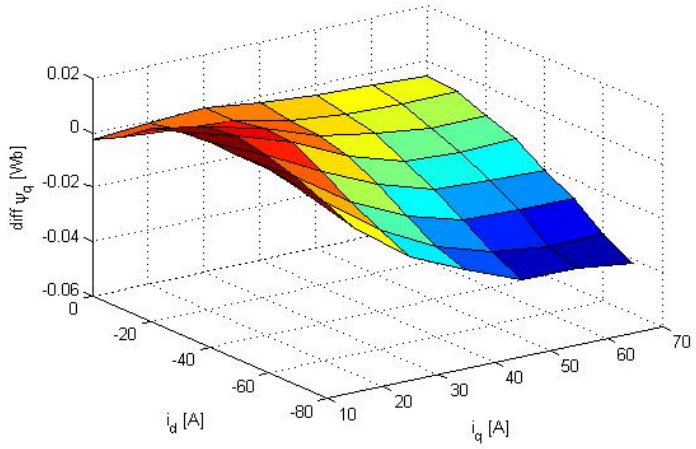

Figure 44: The difference between the real ψ_d and the obtained ψ_d when using the new test method together with open loop sensorless control with compensation.

In figure 45 is the ψ_d in percent shown. It can be concluded that at most current combinations the difference is around -20 to 20 percent.

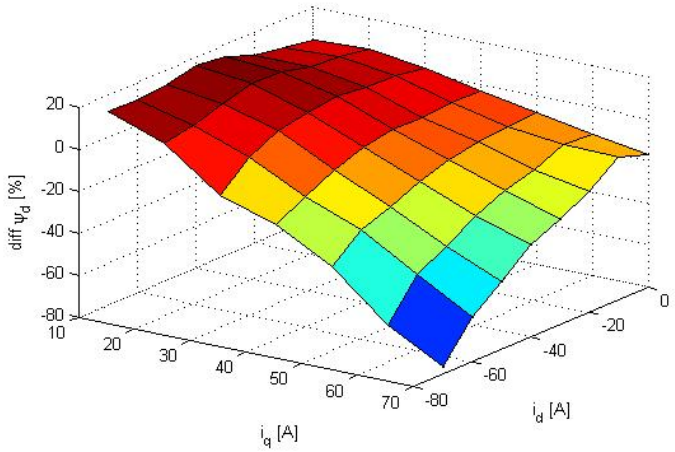

Figure 45: The percentage difference between the real ψ_d and the obtained ψ_d when using the new test method together with open loop sensorless control with compensation.

In figure 46 is the ψ_q difference in percent shown and it can be seen that the difference between the real and obtained flux does not differ more than 20 % in most current combinations.

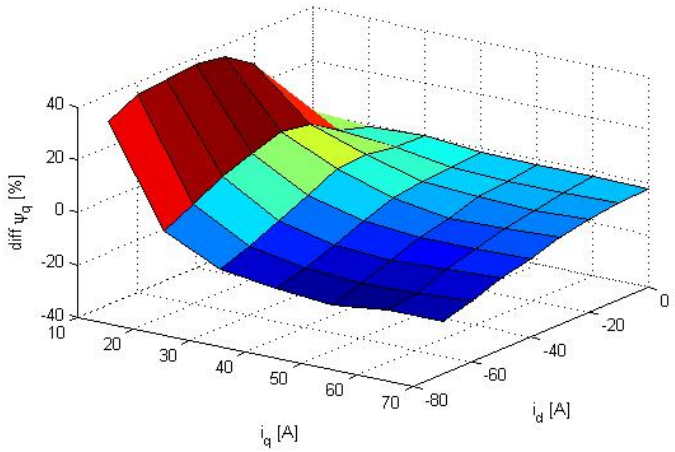

Figure 46: The percentage difference between the real ψ_d and the obtained ψ_d when using the new test method together with open loop sensorless control with compensation.

7 Conclusions

The sensorless control strategies works according to the simulations only for some current combinations and therefor it can not be recommended to use sensorless control when dynamical testing PMSMs.

The pulsating injection sensorless method did not track the rotor position for several current combinations when the PMSM model did not behave linear. Therefor it can be concluded that the lack of performance of the pulsating voltage injection sensorless control method comes from not having a proper saturation effect compensation in the method. In [10] a saturation effect compensation method is presented, but since it requires recording in sensored mode or motor parameters it is not possible to use that compensation method in this set up.

From the results it can be seen that the open loop method is not very sensitive for changes of Ψ_{pm} parameter. From the simulations it is not possible to see any change in the performance of the open loop method when the Ψ_{pm} is changed by multiply it with 0.1 up to 2. When the other parameter L_{sx} is changed it was possible to see changes in the accuracy of the open loop method.

7.1 Is sensorless control useful in the test method?

If the sensorless methods that are used in this simulations can be refined and more carefully adjusted to follow the rotor position more exactly for all current combinations it can be useful for the application. From the simulations that has been conducted it is shown that the sensorless methods are not performing well at all current combinations. It can therefor be concluded that the sensorless methods are not mature enough to be used in the testing application.

If a proper compensation method is developed for the open loop method so the rotor position tracking will be more accurate it can be useful together with the new test method. In [38] a compensation method is presented and it is said that it is mainly depending on the rotor speed thus it is not mentioned if the compensation value has to be changed and individually fitted for each specific electrical motor.

7.2 Future work

In order to make the pulsating injection method perform better it was proposed to use a correctional method for the cross saturation effect on the inductances that comes from the injected high frequent voltage [37]. However that correctional method was built on either knowing the motor parameters or using measured data when the motor was driven with a rotor position sensor, in this case either of the two ways to correctional the rotor position is possible in this application.

However it is possible to obtain flux maps for the PMSM without knowing the motor parameters of the PMSM. With some adjustments in the sensorless

methods like optimizing the phase locked loops and better design of the filters the rotor position can be obtained with higher accuracy and the sensorless dynamic test method can become more useful.

Acknowledgements

Songsong Bao

Sebastian Hall and Gabriel Dominguez.

References

[1] R. Core Writing Team, Pachauri and A. e. Reisinger, *Climate Change 2007: Synthesis Report. Contribution of Working Groups I, II and III to the Fourth Assessment Report of the Intergovernmental Panel on Climate Change*. IPCC, Geneva, Switzerland.

[2] K. D. Schuls M, "Regulation (eu) no 333/2014 of the european parliament and of the council of 11 march 2014 amending regulation (ec) no 443/2009 to define the modalities for reaching the 2020 target to reduce co2 emissions from new passenger cars," *Official journal of the European Union*, no. 5.4.2014, pp. 15–21, 2014.

[3] B. Sweden, "Håll i styrmedlen för fordon med låg klimatpåverkan," *Press release*, 2014.

[4] A. R. Sebastian Hall, Yury Loayza and M. Alaküla, "Consistency analysis of torque measurements performed on a pmsm using dynamic testing," *Not published yet*, 2015.

[5] S. H. Francisco J. Márquez-Fernández and M. Alaküla, "Dynamic testing characterization of a hev traction motor," *Not published yet*, 2015.

[6] R. Krishnan, *Permanent magnet synchronous and brushless DC motor drives [Elektronisk resurs] / R. Krishnan.* Boca Raton : CRC Press/Taylor & Francis, c2010., 2010.

[7] P. Alaküla, M. Karlsson, *Power Electronics, course book.* Department of Industrial Electrical Engineering and Automation, c2013.

[8] A. Rabiei, *Energy Efficiency of an Electric Vehicle Propulsion Inverter Using Various Semiconductor Technologies.* 2013.

[9] D. Lin, P. Zhou, W. Fu, Z. Badics, and Z. Cendes, "A dynamic core loss model for soft ferromagnetic and power ferrite materials in transient finite element analysis.," *IEEE Transactions on Magnetics*, vol. 40, no. 2, pp. 1318 – 1321, 2004.

[10] Y. Li and H. Zhu, "Sensorless control of permanent magnet synchronous motor: a survey.," (Tsinghua Univ. Beijing, Dept. of Electr. Engnieering, Beijing, China), 2008.

[11] R. Bojoi, M. Pastorelli, J. Bottomley, P. Giangrande, and C. Gerada, "Sensorless control of pm motor drives- a technology status review.," (Politecnico di Torino, Dipartimento Energia, Turin, Italy, 19032), 2013.

[12] I. M. Alsofyani and N. Idris, "A review on sensorless techniques for sustainable reliablity and efficient variable frequency drives of induction motors.," *Renewable and Sustainable Energy Reviews*, vol. 24, pp. 111 – 121, 2013.

[13] W. Limei and R. Lorenz, "Rotor position estimation for permanent magnet synchronous motor using saliency-tracking self-sensing method.," *Conference Record of the 2000 IEEE Industry Applications Conference. Thirty-Fifth IAS Annual Meeting World Conference on Industrial Applications of Electrical Energy (Cat. No.00CH37129)*, p. 445, 2000.

[14] S. Shinnaka, "A new speed-varying ellipse voltage injection method for sensorless drive of permanent-magnet synchronous motors with pole saliency - new pll method using high-frequency current component multiplied signal.," *IEEE Transactions on Industry Applications*, vol. 44, no. 3, pp. 777 – 788, 2008.

[15] P. Jansen and R. Lorenz, "Transducerless position and velocity estimation in induction and salient ac machines.," *IEEE Transactions on Industry Applications*, vol. 31, no. 2, pp. 240 – 247, 1995.

[16] M. Corley and R. Lorenz, "Rotor position and velocity estimation for a salient-pole permanent magnet synchronous machine at standstill and high speeds.," *IEEE Transactions on Industry Applications*, vol. 34, no. 4, pp. 784 – 789, 1998.

[17] M. Linke, R. Kennel, and J. Holtz, "Sensorless position control of permanent magnet synchronous machines without limitation at zero speed.," *IEEE 2002 28th Annual Conference of the Industrial Electronics Society. IECON 02*, p. 674, 2002.

[18] J. Holtz, "Acquisition of position error and magnet polarity for sensorless control of pm synchronous machines.," *IEEE Transactions on Industry Applications*, vol. 44, no. 4, pp. 1172 – 1180, 2008.

[19] N. . . . Bianchi, S. . . . Bolognani, J.-H. . . . Jang, and S.-K. . . . Sul, "Comparison of pm motor structures and sensorless control techniques for zero-speed rotor position detection.," *IEEE Transactions on Power Electronics*, vol. 22, no. 6, pp. 2466–2475, 2007.

[20] S. Bolognani, S. Calligaro, R. Petrella, and M. Sterpellone, "Sensorless control for ipmsm using pwm excitation: Analytical developments and implementation issues.," (University of Padova, Department of Electrical Engineering (DIE), Padova, Italy), 2011.

[21] E. Robeischl and M. Schroedl, "Optimized inform measurement sequence for sensorless pm synchronous motor drives with respect to minimum current distortion.," *IEEE Transactions on Industry Applications*, vol. 40, no. 2, pp. 591 – 598, 2004.

[22] S. Ogasawara and H. Akagi, "Implementation and position control performance of a position-sensorless ipm motor drive system based on magnetic saliency.," *IEEE Transactions on Industry Applications*, vol. 34, no. 4, pp. 806 – 812, 1998.

[23] T. Wolbank and J. Machl, "A modified pwm scheme in order to obtain spatial information of ac machines without mechanical sensor.," *APEC. Seventeenth Annual IEEE Applied Power Electronics Conference Exposition (Cat. No.02CH37335)*, p. 310, 2002.

[24] C.-K. Lin, T.-H. Liu, and C.-H. Lo, "Sensorless interior permanent magnet synchronous motor drive system with a wide adjustable speed range.," *IET Electric Power Applications*, vol. 3, no. 2, pp. 133 – 146, 2009.

[25] H.-B. Wang and H.-P. Liu, "A novel sensorless control method for brushless dc motor.," *IET Electric Power Applications*, vol. 3, no. 3, pp. 240 – 246, 2009.

[26] J. Moreira, "Indirect sensing for rotor flux position of permanent magnet ac motors operating over a wide speed range.," *IEEE Transactions on Industry Applications*, vol. 32, no. 6, pp. 1394 – 1401, 1996.

[27] R. Wu and G. Slemon, "A permanent magnet motor drive without a shaft sensor.," *IEEE Transactions on Industry Applications*, vol. 27, no. 5, pp. 1005 – 1011, 1991.

[28] . . Kim, J.-S. (1 and . . Sul, S.-K. (1, "New approach for high-performance pmsm drives without rotational position sensors.," *IEEE Transactions on Power Electronics*, vol. 12, no. 5, pp. 904–911, 1997.

[29] N. Matsui, "Sensorless pm brushless dc motor drives.," *IEEE Transactions on Industrial Electronics*, vol. 43, no. 2, pp. 300 – 308, 1996.

[30] Y.-H. Kim and Y.-S. Kook, "High performance ipmsm drives without rotational position sensors using reduced-order ekf.," *IEEE Power Engineering Review*, vol. 19, no. 1, p. 51, 1999.

[31] K. Hyunbae, M. Harke, and R. Lorenz, "Sensorless control of interior permanent-magnet machine drives with zero-phase lag position estimation.," *IEEE Transactions on Industry Applications*, vol. 39, no. 6, pp. 1726 – 1733, 2003.

[32] C. De Angelo, G. Bossio, J. Solsona, G. Garcia, and M. Valla, "Mechanical sensorless speed control of permanent-magnet ac motors driving an unknown load.," *IEEE Transactions on Industrial Electronics*, vol. 53, no. 2, pp. 406 – 414, 2006.

[33] R. Sepe and J. Lang, "Real-time observer-based (adaptive) control of a permanent-magnet synchronous motor without mechanical sensors.," *IEEE Transactions on Industry Applications*, vol. 28, no. 6, pp. 1345 – 1352, 1992.

[34] S. Bolognani, R. Oboe, and M. Zigliotto, "Sensorless full-digital pmsm drive with ekf estimation of speed and rotor position.," *IEEE Transactions on Industrial Electronics*, vol. 46, no. 1, pp. 184 – 191, 1999.

[35] C. Silva, G. Asher, and M. Sumner, "Hybrid rotor position observer for wide speed-range sensorless pm motor drives including zero speed.," *IEEE Transactions on Industrial Electronics*, vol. 53, no. 2, pp. 373 – 378, 2006.

[36] R. Hejny and R. Lorenz, "Evaluating the practical low-speed limits for back-emf tracking-based sensorless speed control using drive stiffness as a key metric.," *IEEE Transactions on Industry Applications*, vol. 47, no. 3, pp. 1337 – 1343, 2011.

[37] J. M. Liu and Z. Q. Zhu, "Novel sensorless control strategy with injection of high-frequency pulsating carrier signal into stationary reference frame.," *IEEE Transactions on Industry Applications*, vol. 50, no. 4, pp. 2574 – 2583, 2014.

[38] D. Yousfi and M. Adnani, "Indirect position and speed sensing for pmsm sensorless control.," in *7th Internatonal Conference on Power Electronics, ICPE'07*, no. 7th Internatonal Conference on Power Electronics, ICPE'07, (Ecole Nationale des Sciences AppliquÃľes - Marrakech, MESESYP Laboratory, Control Systems, Power Electronics Electric Dives Group), pp. 817–822, 2008.

[39] F. Marquez, *Electric Traction Machine Design for an E-RWD Unit.* PhD thesis, Lund University, 2014.

Nomenclature

α	The injected voltage angle frequency
$\hat{\omega}$	Estimated rotor speed
ω	Rotor rotational speed
Ψ_d	The d-axis stator flux
Ψ_q	The q-axis stator flux
Ψ_{pm}	The flux from the permanent magnets in the PMSM
θ_e	Rotor position estimation
θ_m	Cross saturation effect angle of the rotor
θ_r	Actual rotor position
B_m	Peak magnet flux density
i_d	The d-axis stator current
I_n	Fundamental negative sequence current
I_p	Fundamental positive sequence current
i_q	The q-axis stator current
$i_{\alpha h}$	Current response from the PMSM α axis including the injected voltage
$i_{\beta h}$	Current response from the PMSM β axis including the injected voltage
i_{cd}	D-axis core losses current
i_{cq}	Q-axis core losses current
i_{od}	D-axis magnetization current
i_{oq}	Q-axis magnetization current
i_{ref}	Reference current
J	Rotor moment of inertia
k_c	Eddy current losses constant
k_e	Excess losses constant
k_h	Hysteresis losses constant
L_d	The d-axis inductance
L_q	The q-axis inductance
p	Number of poles in the PMSM
P_{fe}	Core losses in the PMSM model
R_s	The stator resistor
R_{sf}	Equivalent iron loss resistor

T_e Electromagnetic torque

T_{loss} Friction losses

T_{mech} Mechanical torque

u_a The a-phase voltage in a 3-phase system

u_b The b-phase voltage in a 3-phase system

u_c The c-phase voltage in a 3-phase system

u_d The d-axis voltage in the rotating reference frame

u_q The q-axis voltage in the rotating reference frame

u_α The horizontal part of the resulting voltage in stationary reference frame

u_β The vertical part of the resulting voltage in stationary reference frame

u_{hf} The injected high frequency voltage

$v_{\alpha h}$ Injected voltage in α axis

$v_{\beta h}$ Injected voltage in β axis

v_c Injected voltage amplitude

v_{ref} Reference voltage

PMSM Permanent Magnet Synchronous Motor

UNFCCC United Nation Framework Convention on Climate Change